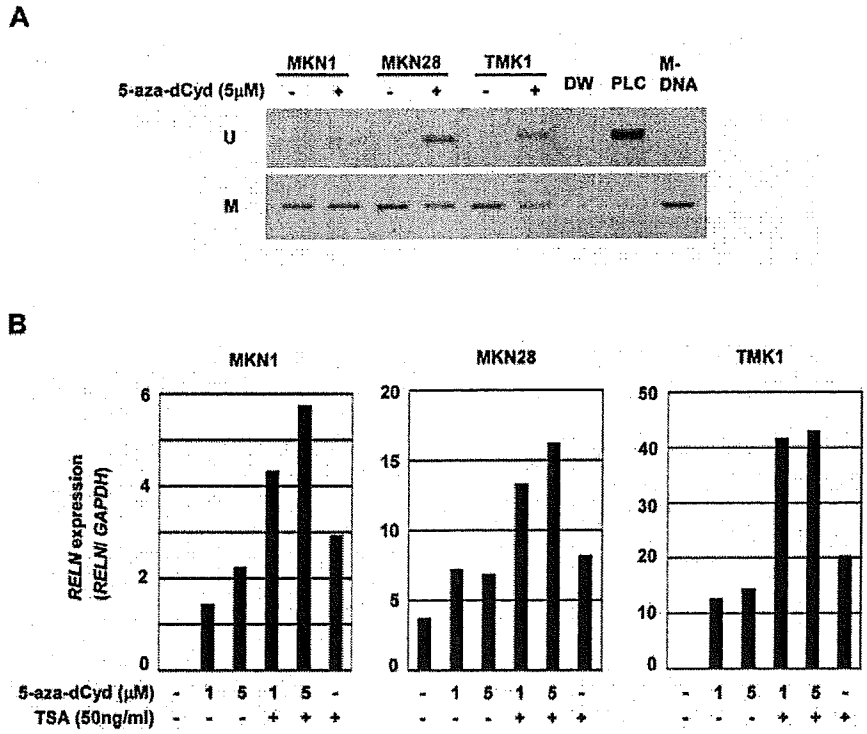

Figure 3. Effect of 5-aza-dCyd and TSA treatment on *RELN* expression. (A) Demethylation of *RELN* in MKN1, MKN28 and TMK1 cells, before and after exposure to 5 μM of 5-aza-dCyd at for 4 days, was analyzed by MSP as described in the legend to Fig. 2. PLC and M-DNA are as in Fig. 2. (B) Expression of *RELN* determined by quantitative real-time RT-PCR in the MKN1, MKN28 and TMK1 cell lines with or without treatment with 5-aza-dCyd (1 or 5 μM) for 4 days and/or TSA (50 ng/ml) for 24 h.

We first assessed the methylation status of a subdomain of the *RELN* CpG island (Fig. 2A) by MSP in the nine GC cell lines lacking *RELN* expression. Seven of the nine cell lines displayed exclusively methylated products, whereas the MKN45 and AZ-521 cells yielded both methylated and unmethylated products (Fig. 2B).

To confirm and quantify the methylation status of *RELN* in these GC cell lines, we next assayed DNA methylation levels of a subdomain of the *RELN* CpG island (Fig. 2A) by the COBRA technique which involves bisulfite PCR followed by restriction enzyme digestion. Consistent with the results of MSP, the *RELN* CpG island was hypermethylated in all of the nine GC cell lines and the MKN45 and AZ-521 cells were partly unmethylated (Fig. 2C). Further analysis of the PCR products by bisulfite-sequencing showed that the CpG island is hypermethylated in two representative GC cell lines (MKN1 and MKN28) that lack *RELN* expression but not in a non-tumor gastric epithelial tissue (5NT) (Fig. 2D). Taken together, these data show that the *RELN* CpG island is frequently hypermethylated in GC cells.

Role of DNA methylation and histone deacetylation in the silencing of RELN expression in GC cells. To investigate the role of methylation of the *RELN* CpG island in silencing of the *RELN* gene, we assayed the effect of demethylation of the *RELN* CpG island on the expression of *RELN* mRNA. Three of the GC cell lines that lack *RELN* expression (MKN1, MKN28 and TMK1) were therefore treated with 5-aza-dCyd, a methyltransferase inhibitor, following which RELN mRNA expression was assayed by quantitative real-time RT-PCR. Demethylation of the *RELN* CpG island was observed by PCR analysis (Fig. 3A) and was accompanied by restoration of the expression of *RELN* mRNA in all three cell lines (Fig. 3B). These data implied that methylation of the *RELN* CpG island silences *RELN* mRNA expression.

We additionally observed elevated expression of *RELN* mRNA after treatment with the histone deacetylase inhibitor, TSA, and TSA treatment also enhanced expression of *RELN* mRNA by 5-aza-dCyd in all three cell lines (Fig. 3B). These findings suggested that histone deacetylation may also contribute to transcriptional silencing of *RELN*.

Defective expression of the RELN protein in primary GC tumors. To determine whether the silencing of *RELN* that was observed in the GC cell lines was relevant for primary human carcinomas, we compared the expression of the RELN protein in 25 primary GC samples with that of the respective non-tumor tissue by immunohistochemistry. The results of the immunostaining of RELN are summarized in Table II, and representative images are shown in Fig. 4. The RELN protein was strongly expressed in the cytoplasm of all non-tumor gastric epithelia (Fig. 4A-D). In contrast, expression of RELN was weak or absent in GC tumors (Fig. 4E-H). For all of the GCs, the expression of RELN was lower in the tumors than in their non-tumor counterparts (Table II). When RELN was detected in GC cells, it also localized in the cytoplasm.

To clarify the relationship between the level of the RELN protein in GC tumors and various clinicopathological para-

Table II. Expression levels of RELN protein in paired tumor tissues and non-tumor tissues from 25 patients with GC.

	RELN protein expression[a]		
Tissue	2+	1+	-
Non-tumor	25 (100%)	0	0
Tumor	0	15 (60%)	10 (40%)

[a]2+, strong; 1+, weak; -, absent.

meters, we correlated RELN expression with available clinical data from the 25 patients. For this analysis the patients were divided into two groups based on whether the expression of the RELN protein was weak or absent (Table III). Absence of RELN expression significantly correlated with advanced tumor stage (stage III or IV).

Methylation of RELN in primary GC tumors. To determine whether the methylation of the *RELN* CpG island observed in GC cell lines also occurs in primary human carcinomas, we assessed the methylation status of RELN in paired tumor and non-tumor tissues from an additional 15 patients with primary GC and in three normal gastric epithelial tissues by COBRA. Twelve of the 15 patients were positive for *H. pylori*. All 15 of the non-tumor gastric mucosal samples were from patients that had endoscopically documented atrophic gastritis. Methylation of *RELN* was observed in all 15 GC tumors and in 12 of the 15 non-tumor gastric epithelial tissues, but not in any of the three normal gastric epithelial tissues (Fig. 5A). Although methylation of *RELN* was found in both GC tumors

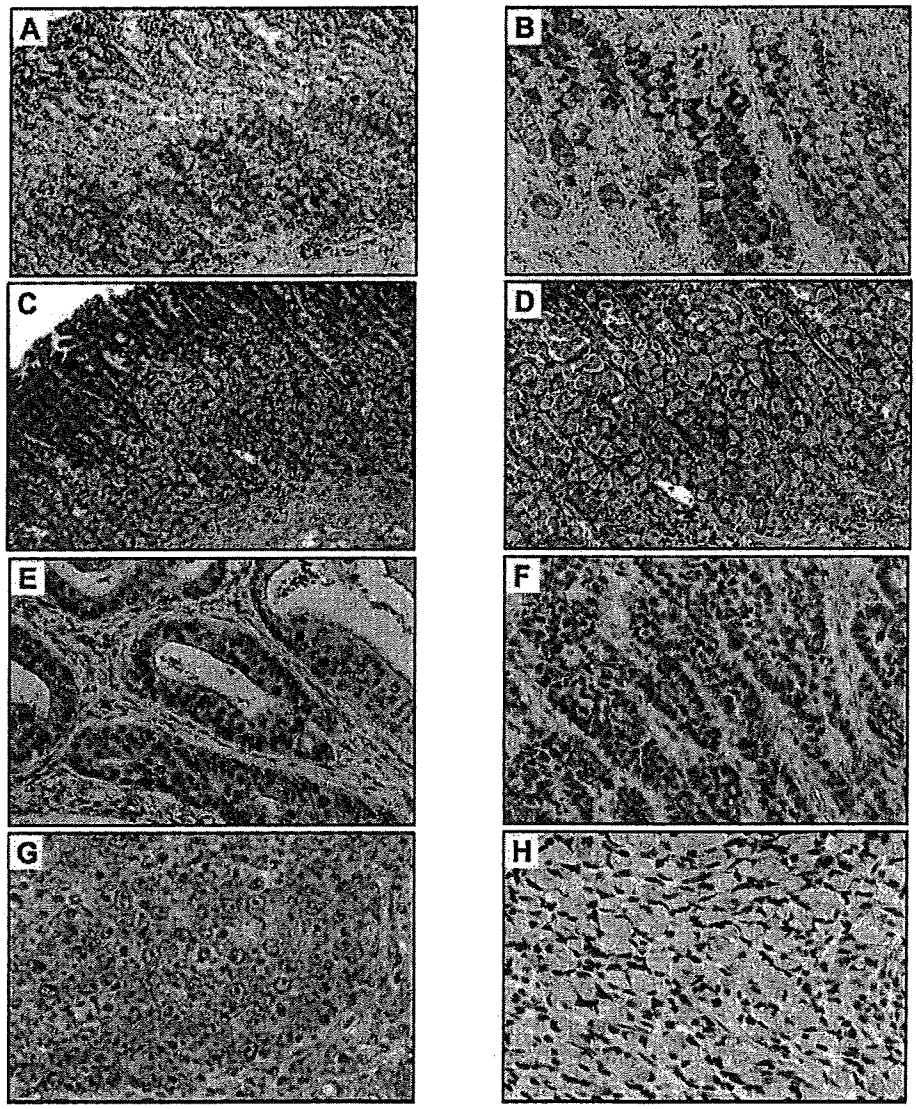

Figure 4. Representative immunostaining of RELN in non-tumor gastric epithelia and in primary GC tumors. (A and B) Immunostaining (brown color) of RELN in non-tumor gastric epithelia at low (A, x40) and high (B, x200) magnification. (C and D) Hematoxylin and eosin staining of the same specimens shown in (A) and (B), respectively. (E-H) Immunostaining of RELN in primary GC tumors: intestinal type (E and F) and diffuse type (G and H). Expression of RELN was weak (E and G) or absent (F and H) in primary GC tumors. Original magnification x200.

Table III. Relationship between levels of expression of RELN protein and clinicopathological features in 25 primary GCs.

Features	n	RELN expression[a] 1+ (n=15)	- (n=10)	P-value[c]
Age				
≤70	12	7	5	0.89
>70	13	8	5	
Gender				
Male	17	12	5	0.13
Female	8	3	5	
Histological type[b]				
Intestinal type	13	9	4	0.28
Diffuse type	12	6	5	
Stage (TNM)				
Stage I/II	17	13	4	0.01
Stage III/IV	8	2	6	
Lymph node metastasis				
(-)	12	9	3	0.14
(+)	13	6	7	

[a]1+, weak; -, absent. [b]Lauren's histological classification. [c]$\chi 2$ test.

and in non-tumor tissues, the level of *RELN* methylation was significantly higher in 13 of the 15 tumors when compared with their non-tumor tissue counterparts (Wilcoxon signed-rank test, P=0.001) (Fig. 5B). These findings are consistent with the results of immunohistochemistry that indicate that the expression of RELN is reduced in tumors compared with their non-tumor counterparts.

Discussion

This is the first report that *RELN* is silenced in GC by aberrant promoter hypermethylation and we have demonstrated this silencing by a number of approaches. Thus, all nine GC cell lines assayed lacked the expression of *RELN* mRNA. Furthermore, methylation assays of GC cells by MSP, COBRA, bisulfite-sequencing and 5-aza-dCyd and TSA drug treatment, indicated that a CpG island in the 5' promoter region of *RELN*, is hypermethylated. Methylation of the *RELN* CpG island was found not only in GC cell lines but also in all 15 primary GCs examined. Moreover, the expression of the RELN protein was weak or absent in primary GC tumors and RELN expression level was significantly reduced in tumors compared with their non-tumor counterparts. Our data further suggest that silencing of RELN is associated with the progression of GC since the absence, rather than the weak expression, of RELN significantly correlated with a more advanced stage of primary GC. The combined results indicate that methylation

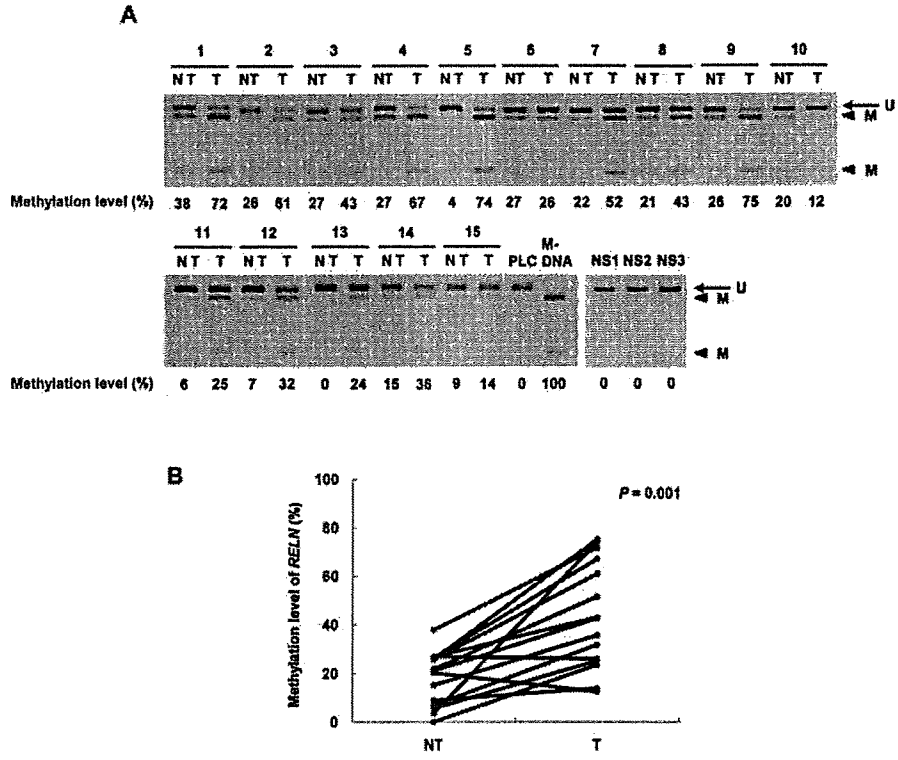

Figure 5. Analysis of *RELN* methylation in paired tumor and non-tumor tissues. (A) COBRA of *RELN* in paired tumor (T) and non-tumor (NT) tissues from 15 patients with primary GC and from three normal gastric epithelia (NS). The arrow and arrowheads indicate undigested products (U, unmethylated DNA) and digested fragments (M, methylated DNA), respectively. Methylation levels of *RELN* were determined as described in Materials and methods and are expressed as a percentage of the methylated DNA (M-DNA) positive control value. The value obtained for normal peripheral lymphocytes (PLC) was used as the baseline (0%). (B) Plot of the methylation levels of *RELN* in paired tumors (T) and non-tumor tissues (NT) from 15 patients with primary GCs. The level of *RELN* methylation was significantly higher in tumors when compared with their non-tumor tissue counterparts (Wilcoxon signed-rank test, P=0.001).

of the *RELN* promoter contributes to the silencing of the *RELN* gene and that silencing of the RELN gene plays a role in GC tumor progression. However, the number of primary GC samples examined in this study was relatively small. Furthermore, it was not possible to directly determine the correlation between levels of expression and methylation of *RELN* in primary GCs due to the small amount of total RNA that was obtained from the biopsy samples. Therefore, further studies using a larger number of primary samples are required to clarify the exact relationship between methylation and RELN expression in primary GCs.

Interestingly, methylation of *RELN* was also observed in most of the non-tumor gastric epithelial tissues examined, although levels of *RELN* methylation in non-tumor gastric epithelial tissues were lower than those observed in GC tumors. All of the non-tumor gastric mucosa showed atrophic gastritis, and most of the patients from whom the samples were taken were infected with *H. pylori*, the major cause of chronic gastritis which leads to atrophic changes in the gastric mucosa (26). Most GCs arise on a background of atrophic gastritis (27). These findings suggest that methylation of *RELN* occurs in precancerous atrophic gastritis and is enhanced during the development and progression of GC.

Our immunohistochemical analyses, combined with the histological examinations, suggested that RELN is expressed mainly in the pepsinogen-secreting chief cells of gastric epithelia. The physiological function of RELN in the stomach is currently unclear but is an important issue for future studies.

To date, varying levels of RELN expression have been reported in cancers. High expression of RELN was reported in 87.5% of esophageal cancers (28) and in 39% of prostate cancers (29). Conversely, the expression of RELN was reported to be only focal or completely absent in 72% of pancreatic cancers in which the *RELN* promoter was hypermethylated (14). Although the functional role of RELN in tumorigenesis remains largely unknown, knockdown of *RELN* in pancreatic cancer cells by small interfering RNA resulted in enhanced cell mobility, invasiveness and colony-forming ability (14). These findings suggest the possibility that the loss of RELN might enhance cell metastasis. Clearly further studies are required to fully understand the role of RELN in tumorigenesis.

In conclusion, the expression of RELN is lost or highly reduced by aberrant promoter hypermethylation in GCs. Although the exact mechanism by which RELN contributes to tumorigenicity remains to be elucidated, the data presented in this study, together with the recent finding that the *VLDLR* gene, whose product functions as the receptor for RELN, is also epigenetically silenced in GC (9), clearly suggest that disruption of the RELN pathway is involved in gastric carcinogenesis.

References

1. Ferlay J, Bray F, Pisani P and Parkin DM: GLOBOCAN 2000: Cancer Incidence, Mortality, and Prevalence Worldwide. Version 1.0. Vol. 5. IARC Press, Lyon.
2. Baylin SB, Herman JG, Graff JR, Vertino PM and Issa JP: Alterations in DNA methylation: a fundamental aspect of neoplasia. Adv Cancer Res 72: 141-196, 1998.
3. Ushijima T and Sasako M: Focus on gastric cancer. Cancer Cell 5: 121-125, 2004.
4. D'Arcangelo G, Miao GG, Chen SC, Soares HD, Morgan JI and Curran T: A protein related to extracellular matrix proteins deleted in the mouse mutant reeler. Nature 374: 719-723, 1995.
5. Curran T and D'Arcangelo G: Role of reelin in the control of brain development. Brain Res Brain Res Rev 26: 285-294, 1998.
6. Tissir F and Goffinet AM: Reelin and brain development. Nat Rev Neurosci 4: 496-505, 2003.
7. Trommsdorff M, Gotthardt M, Hiesberger T, Shelton J, Stockinger W, Nimpf J, Hammer RE, Richardson JA and Herz J: Reeler/Disabled-like disruption of neuronal migration in knockout mice lacking the VLDL receptor and ApoE receptor 2. Cell 97: 689-701, 1999.
8. Howell BW, Hawkes R, Soriano P and Cooper JA: Neuronal position in the developing brain is regulated by mouse disabled-1. Nature 389: 733-737, 1997.
9. Takada H, Imoto I, Tsuda H, Nakanishi Y, Sakakura C, Mitsufuji S, Hirohashi S and Inazawa J: Genomic loss and epigenetic silencing of very-low-density lipoprotein receptor involved in gastric carcinogenesis. Oncogene 25: 6554-6562, 2006.
10. De Silva U, Arcangelo GD, Braden VV, Chen J, Miao GG, Curran T and Green ED: The human reelin gene: isolation, sequencing, and mapping on chromosome 7. Genome Res 7: 157-164, 1997.
11. Chen Y, Sharma RP, Costa RH, Costa E and Grayson DR: On the epigenetic regulation of the human reelin promoter. Nucleic Acids Res 30: 2930-2939, 2002.
12. Abdolmaleky HM, Cheng KH, Russo A, Smith CL, Faraone SV, Wilcox M, Shafa R, Glatt SJ, Nguyen G, Ponte JF, Thiagalingam S and Tsuang MT: Hypermethylation of the reelin (RELN) promoter in the brain of schizophrenic patients: a preliminary report. Am J Med Genet B Neuropsychiatr Genet 134: 60-66, 2005.
13. Grayson DR, Jia X, Chen Y, Sharma RP, Mitchell CP, Guidotti A and Costa E: Reelin promoter hypermethylation in schizophrenia. Proc Natl Acad Sci USA 102: 9341-9346, 2005.
14. Sato N, Fukushima N, Chang R, Matsubayashi H and Goggins M: Differential and epigenetic gene expression profiling identifies frequent disruption of the RELN pathway in pancreatic cancers. Gastroenterology 130: 548-565, 2006.
15. Hojo H: Establishiment of cultured cell lines of human stomach cancer - origin and their morphological characteristics (in Japanese). Niigata Igakukai Zasshi 91: 737-752, 1977.
16. Motoyama T, Hojo H and Watanabe H: Comparison of seven cell lines derived from human gastric carcinomas. Acta Pathol Jpn 36: 65-83, 1986.
17. Ochiai A, Yasui W and Tahara E: Growth-promoting effect of gastrin on human gastric carcinoma cell line TMK-1. Jpn J Cancer Res 76: 1064-1071, 1985.
18. Akiyama S, Amo H, Watanabe T, Matsuyama M, Sakamoto J, Imaizumi M, Ichihashi H, Kondo T and Takagi H: Characteristics of three human gastric cancer cell lines, NU-GC-2, NU-GC-3 and NU-GC-4. Jpn J Surg 18: 438-446, 1988.
19. Park JG, Frucht H, La Rocca RV, Bliss DP Jr, Kurita Y, Chen TR, Henslee JG, Trepel JB, Jensen RT, Johnson BE, Bang YJ, Kim JP and Gazdar AF: Characteristics of cell lines established from human gastric carcinoma. Cancer Res 50: 2773-2780, 1990.
20. Sekiguchi M, Sakakibara K and Fujii G: Establishment of cultured cell lines derived from a human gastric carcinoma. Jpn J Exp Med 48: 61-68, 1978.
21. Takada H, Imoto I, Tsuda H, Sonoda I, Ichikura T, Mochizuki H, Okanoue T and Inazawa J: Screening of DNA copy-number aberrations in gastric cancer cell lines by array-based comparative genomic hybridization. Cancer Sci 96: 100-110, 2005.
22. Price AB: The Sydney System: histological division. J Gastroenterol Hepatol 6: 209-222, 1991.
23. Xiong Z and Laird PW: COBRA: a sensitive and quantitative DNA methylation assay. Nucleic Acids Res 25: 2532-2534, 1997.
24. Lauren P: The two histological main types of gastric carcinoma: diffuse and so-called intestinal-type carcinoma. an attempt at a histo-clinical classification. Acta Pathol Microbiol Scand 64: 31-49, 1965.

25. Japanese Gastric Cancer Association: Japanese Classification of Gastric Carcinoma - 2nd English edition. Gastric Cancer 1: 10-24, 1998.
26. Asaka M, Kimura T, Kudo M, Takeda H, Mitani S, Miyazaki T, Miki K and Graham DY: Relationship of Helicobacter pylori to serum pepsinogens in an asymptomatic Japanese population. Gastroenterology 102: 760-766, 1992.
27. El-Zimaity H: Gastritis and gastric atrophy. Curr Opin Gastroenterol 24: 682-686, 2008.
28. Wang Q, Lu J, Yang C, Wang X, Cheng L, Hu G, Sun Y, Zhang X, Wu M and Liu Z: CASK and its target gene Reelin were co-upregulated in human esophageal carcinoma. Cancer Lett 179: 71-77, 2002.
29. Perrone G, Vincenzi B, Zagami M, Santini D, Panteri R, Flammia G, Verzi A, Lepanto D, Morini S, Russo A, Bazan V, Tomasino RM, Morello V, Tonini G and Rabitti C: Reelin expression in human prostate cancer: a marker of tumor aggressiveness based on correlation with grade. Mod Pathol 20: 344-351, 2007.

ANTICANCER RESEARCH *29*: 4989-4994 (2009)

Infrequent Amplification of *JUN* in Hepatocellular Carcinoma

MIO ENDO[1], KOHICHIROH YASUI[1], TOMOAKI NAKAJIMA[1], YASUYUKI GEN[1], KAZUHIRO TSUJI[1], OSAMU DOHI[1], KEIKA ZEN[1], HIRONORI MITSUYOSHI[1], MASAHITO MINAMI[1], YOSHITO ITOH[1], MASAFUMI TANIWAKI[2], SHINJI TANAKA[3], SHIGEKI ARII[3], TAKESHI OKANOUE[1,4] and TOSHIKAZU YOSHIKAWA[1]

Department of [1]Molecular Gastroenterology and Hepatology, and [2]Molecular Hematology and Oncology, Graduate School of Medical Science, Kyoto Prefectural University of Medicine, Kyoto; [3]Department of Hepato-Biliary-Pancreatic Surgery, Tokyo Medical and Dental University, Tokyo; [4]Center of Gastroenterology and Hepatology, Saiseikai Suita Hospital, Suita, Japan

Abstract. *Aim: To determine whether JUN (the oncogene encoding c-Jun protein) is amplified and overexpressed in hepatocellular carcinoma (HCC). Materials and Methods: DNA copy number aberrations were investigated using a high-density oligonucleotide microarray. DNA copy numbers were determined by fluorescence in situ hybridization. Genomic DNA and mRNA were quantified using real-time quantitative PCR. Results: A novel amplification was found at the chromosomal region 1p32-31 in a JHH-2 HCC cell line within which JUN is amplified and overexpressed. However, no copy number gain of JUN (>2-fold) was observed in 34 primary HCC tumors. Rather, a loss of JUN (<0.5-fold) was seen in 13 (38%) out of the 34 tumors and expression of JUN was significantly lower in 26 (70%) out of the 37 HCC tumors compared with their nontumorous counterparts. Conclusion: Although JUN was amplified and overexpressed in JHH-2 HCC cells, amplification and overexpression of JUN may be rare in primary HCCs.*

Hepatocellular carcinoma (HCC) is the fifth most common malignancy in men and the eighth most common in women worldwide and is estimated to cause approximately half a million deaths annually (1). Although the risk factors for HCC are well characterized, the molecular pathogenesis of this widespread type of cancer remains poorly understood (2). Amplification of DNA in specific chromosomal regions plays a crucial role in the development and progression of human malignancies, specifically when proto-oncogenic target genes within those amplicons are overexpressed. To identify genes potentially involved in HCC, we investigated DNA copy number aberrations in human HCC cell lines using high resolution single nucleotide polymorphism (SNP) arrays (3-5). We found that a novel amplification at the chromosomal region 1p32-31 occurs in HCC cell line and that the human oncogene *JUN*, which lies within the 1p32-31 amplicon, is amplified and overexpressed.

The oncogene *JUN* encodes the protein c-Jun, a component of the AP-1 transcriptional complex which regulates a wide range of cellular processes, including cell proliferation, death, survival and differentiation (6-8). *JUN* is the cellular homologue of *v-Jun*, the transforming oncogene of the avian sarcoma virus 17 (9, 10). Many experimental approaches have indicated that *JUN* plays an important role in carcinogenesis. Thus, *JUN* can transform mammalian cells, when coexpressed with an activated oncogene such as *Ras* or *Src* (11). Furthermore, transgenic mice expressing *JUN* develop osteosarcoma in cooperation with c-Fos (12). Recently, several lines of evidence have suggested that *JUN* is implicated in human cancer, including highly aggressive sarcomas (13), Hodgkin lymphomas (14) and acute myeloid leukemia (15). Amplification of *JUN* has also recently been described in highly aggressive sarcomas (13) and malignant pleural mesotheliomas (16). Most important in terms of this study, *JUN* also appears to be crucial for initiation of HCC development in a mouse model (17).

Therefore, overexpression of *JUN* following amplification may contribute to the initiation or progression of cancer, including HCC. In this study, based on the findings of the SNP-array analysis, we determined if *JUN* is indeed amplified and overexpressed in primary HCC tumors.

Materials and Methods

Cell lines and tumor samples. A total of 21 liver cancer cell lines (HCC-derived HLE, HLF, PLC/PRF/5, Li7, Huh7, Hep3B, SNU354, SNU368, SNU387, SNU398, SNU423, SNU449, SNU475, JHH-1, JHH-2, JHH-4, JHH-5, JHH-6, JHH-7, Huh1,

Correspondence to: Dr. Kohichiroh Yasui, Department of Molecular Gastroenterology and Hepatology, Graduate School of Medical Science, Kyoto Prefectural University of Medicine, 465 Kajii-cho, Kamigyo-ku, Kyoto 602-8566, Japan. Tel: +81 752515519, Fax: +81 752510710, e-mail: yasuik@koto.kpu-m.ac.jp

Key Words: Gene amplification, hepatocellular carcinoma, *JUN*.

0250-7005/2009 $2.00+.40

and the hepatoblastoma line HepG2) were obtained from the Health Science Research Resources Bank (Osaka, Japan) and the American Type Culture Collection (Manassas, VA, USA) and were examined as described previously (3). All cell lines were maintained in Dulbecco's modified Eagle's medium supplemented with 10% fetal calf serum. Paired tumor and nontumor tissues were obtained from 37 HCC patients who underwent surgery at the Hospital of Tokyo Medical and Dental University. All specimens were frozen immediately in liquid nitrogen and stored at −80°C until required. Genomic DNA was isolated using the Puregene DNA isolation kit (Gentra, Minneapolis, MN, USA) and total RNA was obtained using Trizol reagent (Invitrogen, Carlsbad, CA, USA). Thirty-four tumor samples were available for DNA analyses, and 37 paired tumor and nontumor samples were available for mRNA analyses. Prior to the study, informed consent was obtained and the study was approved by Ethics Committees.

SNP array. DNA copy number changes were analyzed by the GeneChip Mapping 100K array (Affymetrix, Santa Clara, CA, USA), as described previously (3). Copy number changes were calculated using the Copy Number Analyzer for Affymetrix GeneChip Mapping Arrays (CNAG; http://www.genome.umin.jp; (18).

Fluorescence in situ hybridization (FISH). FISH was performed using three bacterial artificial chromosomes (BACs), RP11-1040N24, RP11-63G10 and RP11-960H15 as probes (Invitrogen), as described previously (3). The BACs were selected based on their homology to locations in the human genome according to the database provided by the UCSC (http://genome.ucsc.edu/).

Real-time quantitative PCR. Genomic DNA and mRNA were quantified using a real-time fluorescence detection method, as described previously (3). The primers used were as follows: *JUN* DNA forward: 5'-CAGGTGGCACAGCTTAAACA-3', reverse: 5'-TTTTTCTCTCCGTCGCAACT-3'; *JUN* mRNA forward: 5'-CCCCAAGATCCTGAAACAGA-3', reverse: 5'-CCGTTGCTGGA CTGGATTAT-3'. These primers were designed using Primer3Plus (http://www.bioinformatics.nl/cgi-bin/primer3plus/ primer3plus.cgi) on the basis of sequence data obtained from the NCBI database (http://www.ncbi.nlm.nih.gov/). Endogenous controls for mRNA and genomic DNA levels were *GAPDH* and long interspersed nuclear element 1 (*LINE-1*), respectively.

Statistical analysis. All statistical analyses were performed using SPSS 15.0 software (SPSS Inc., Chicago, IL, USA). The Wilcoxon signed-rank test was used to compare *JUN* mRNA levels between tumorous and non-tumorous tissues. *P*-values of <0.05 were considered significant.

Results

Detection of 1p32-31 amplification in a JHH-2 HCC cell line by array analyses. Twenty HCC cell lines were screened for DNA copy number aberrations using Affymetrix GeneChip Mapping 100K array analysis. One of the 20 cell lines, JHH-2, exhibited a high-level copy-number gain that is indicative of gene amplification within the chromosomal region 1p32-31 (Figure 1A). The estimated extent of the region of amplification was 3.9 Mb. This chromosomal region lies between the Affymetrix markers SNP_A-1693528 and SNP_A-1722104 and contains 27 known or predicted protein-coding genes including *JUN* (Figure 1B). To confirm amplification of *JUN*, we performed FISH analyses on JHH-2 cells using the BACs RP11-1040N24, RP11-63G10 and RP11-960H15 as probes. The BAC RP11-63G10, which contains *JUN*, generated an amplified FISH signal (Figure 1D). In contrast, neither of the BACs RP11-1040N24 or RP11-960H15, which correspond to chromosomal regions outside of the amplicon, showed an amplified signal (Figure 1C and E).

DNA copy number and expression of JUN in liver cancer cell lines. Amplification of *JUN* was further determined by assay of the DNA copy number of *JUN* in 21 liver cancer cell lines (20 HCC cell lines and the hepatoblastoma line HepG2) by real-time quantitative PCR. For this analysis, the copy number values were normalized by assigning the copy number of genomic DNA derived from normal lymphocytes a value of 1. Copy number changes were counted as gains or losses if the copy number value for a given tumor cell was >2.0 or <0.5, respectively. A copy number gain-of-*JUN* was observed in 3 out of the 21 cell lines: JHH-2, JHH-7 and PLC/PRF/5 (Figure 2A). Loss of *JUN* was observed in 1 out of the 21 cell lines: Huh7 (Figure 2A).

A common criterion for the designation of a gene as a putative target of amplification is that its gene amplification leads to its overexpression (19). To determine whether gene amplification leads to overexpression of *JUN*, we assayed the mRNA level of *JUN* in the same 21 liver cancer cell lines by real-time quantitative PCR. *JUN* mRNA was overexpressed in 2 out of the 3 cell lines (JHH-2 and JHH-7 but not PLC/PRF/5) that had copy number gains of the *JUN* gene (Figure 2B). These findings suggested that *JUN* could be the target of the 1p32-31 amplicon.

DNA copy number and expression of JUN in primary HCC tumors. To determine if the amplification and overexpression of *JUN* that was observed in HCC cell lines was relevant to primary human carcinomas, we first determined the copy number of *JUN* in 34 primary HCCs using a similar method to that used for the HCC cell lines. No copy number gain of *JUN* (>2-fold) was observed in any of the tumors. Instead, a loss of *JUN* (<0.5-fold) was seen in 13 (38%) out of the 34 tumors (Figure 3A).

We next further assayed the mRNA level of *JUN* in paired tumor and nontumor tissues from 37 HCC patients (Figure 3B). The expression of *JUN* was significantly lower in 26 (70%) of the tumors compared with their nontumorous counterparts (Wilcoxon signed-rank test; p=0.002).

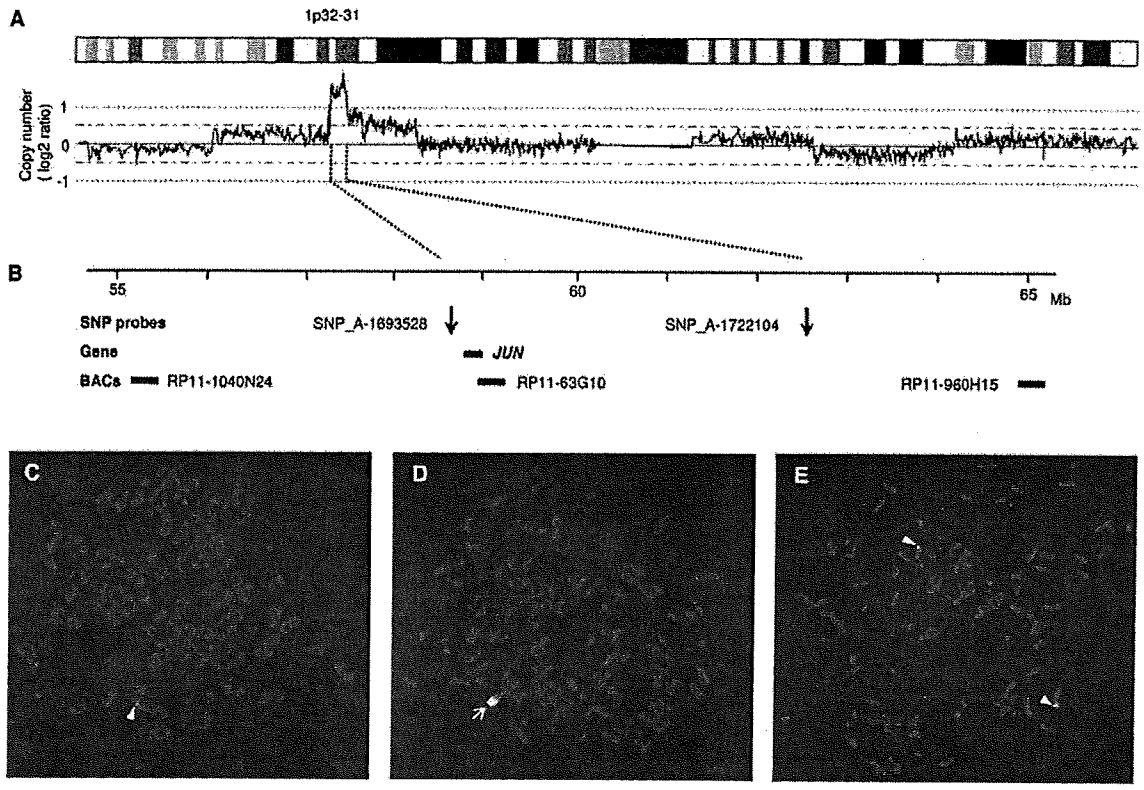

Figure 1. *Map of the amplicon at 1p32-31 in the JHH-2 cell line. A, Copy number profiles for chromosome 1 in JHH-2 cells. Copy number values were determined by SNP array analyses. B, The position of the Affymetrix SNP probes, the JUN gene and the three BACs chosen as probes for the FISH experiment based on the UCSC genome database (http://genome.ucsc.edu/) is shown. C-E, Representative images of FISH on metaphase chromosomes from JHH-2 cells using the following BAC probes: RP11-1040N24 (C), RP11-63G10 (D) and RP11-960H15 (E). RP11-63G10 shows an amplified signal (arrow; D), while RP11-1040N24 and RP11-960H15 show one copy and two copies per cell, respectively (arrowheads; C and E).*

Discussion

In the present study, we show that *JUN* is amplified and overexpressed in the JHH-2 HCC cell line. This cell line is derived from a Japanese HCC patient who was seronegative for hepatitis B virus (HBV) surface antigen (20). Furthermore, a copy number gain of *JUN* (>2-fold) was observed in 3 out of the 21 liver cancer cell lines (including JHH-2) that were tested and 2 of these 3 cell lines (JHH-2 and JHH-7) also showed enhanced mRNA expression of *JUN*. However, no copy number gain of *JUN* was observed in 34 primary HCC tumors that were examined. In fact, loss of *JUN* (<0.5-fold) was seen in 13 (38%) out of the 34 tumors. This loss of *JUN* in primary HCCs is consistent with previous studies that identified a frequent loss of DNA in HCCs at the chromosomal location where *JUN* resides (1p32-31) in comparative genomic hybridization and DNA microarray studies (21, 22). These findings suggest that amplification of *JUN* is rare in primary HCCs. However, the number of primary tumor samples examined in this study was relatively small. Further analysis of a greater number of primary samples is required to confirm the status of *JUN* amplification in primary HCCs.

The overall levels of the *JUN* protein product c-Jun are regulated by transcriptional and translational mechanisms and fine-tuning is achieved by post-translational modification, primarily by phosphorylation (23). Our analysis focused on *JUN* mRNA levels and further study is required to determine the mechanism and functional significance of the regulation of c-Jun protein levels in HCC. Real-time quantitative PCR analyses of primary HCC samples showed that expression of *JUN* mRNA is lower in tumors than in their nontumorous counterparts. These data are consistent with the fact that *JUN* is usually not overexpressed in human tumors (7). However, the low level of *JUN* in tumors does not necessarily imply that *JUN* does not have oncogenic potential in HCC. Several lines of evidence demonstrate a liver-specific function of *JUN* for cell survival and cell-cycle progression. *JUN* is essential for normal hepatogenesis during embryonic development (24, 25). Differentiated hepatocytes also require *JUN* for cell-cycle

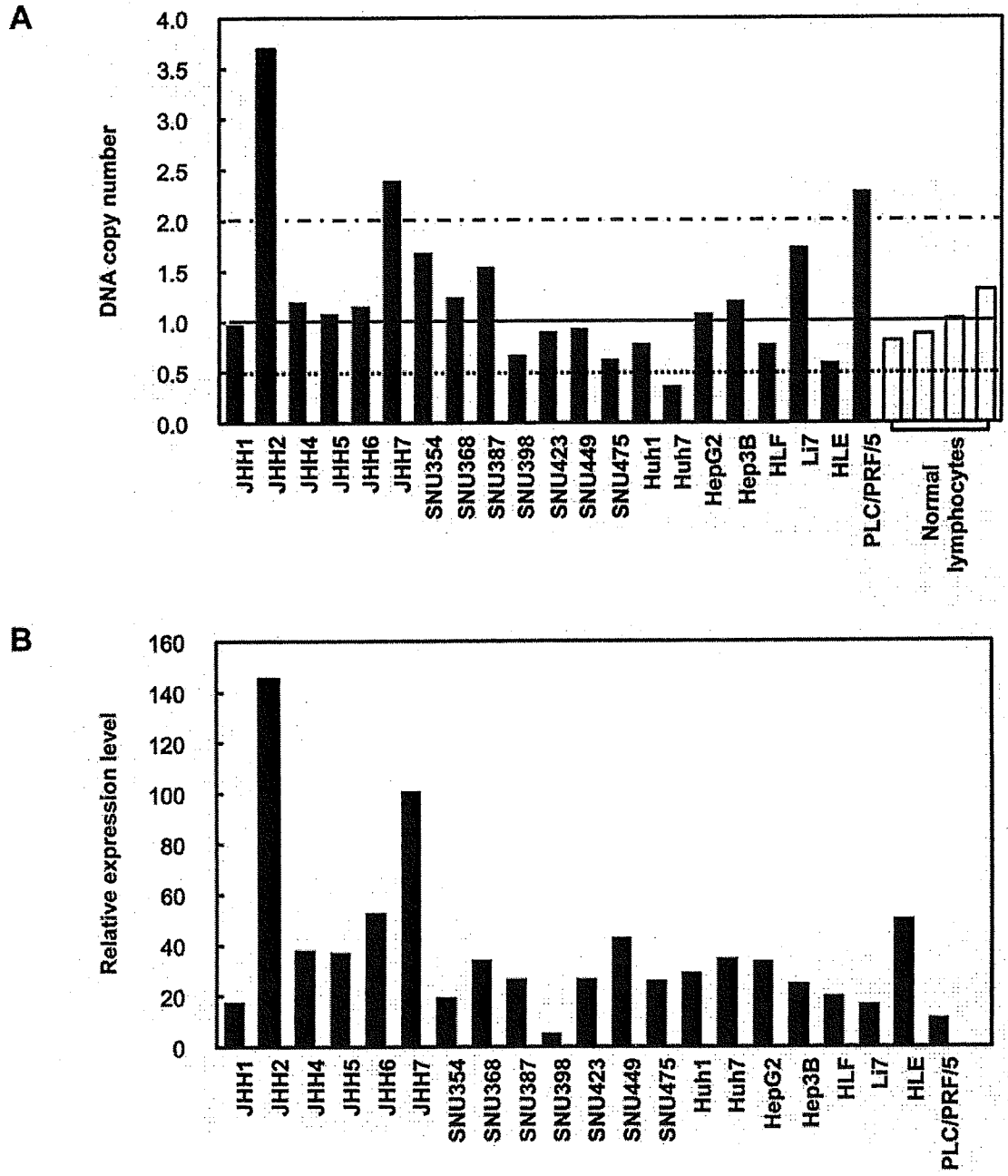

Figure 2. *DNA copy number and expression of JUN in liver cancer cell lines. A, DNA copy number of JUN in 21 liver cancer cell lines (20 HCC cells and one hepatoblastoma line HepG2) and four different peripheral blood lymphocyte samples (normal cell controls) was evaluated by real-time quantitative PCR with reference to LINE-1 controls. Values are normalized such that the average copy number in genomic DNA derived from normal lymphocytes has a value of 1 (solid horizontal line). A value greater than the cut-off value of 2, which represents a twofold increase in copy number over that of normal lymphocytes, was used to determine copy number gain and is shown as a broken line. A value less than the cut-off value of 0.5, which represents one half of the copy number of normal lymphocytes, was used to determine copy number loss and is shown as a dotted line. B, Relative expression levels of JUN in 21 liver cancer cell lines, as evaluated by real-time quantitative PCR, are shown. The results are presented as a ratio between the expression level of JUN and a reference gene (GAPDH) to correct for variation in the amount of RNA.*

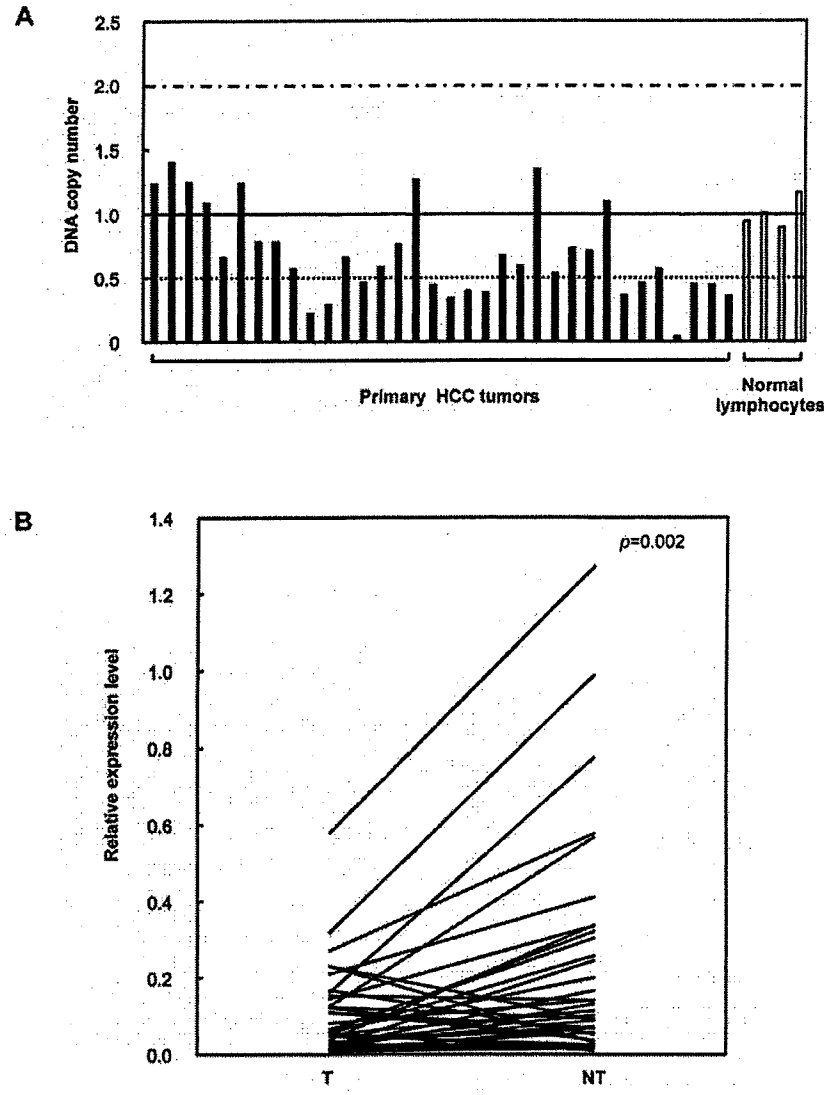

Figure 3. *DNA copy number and expression level of JUN in primary HCC tumors. A, The copy number of JUN in 34 primary HCC tumors and four normal peripheral blood lymphocyte samples was determined as described in the Materials and Methods Section. B, The relative expression of JUN in paired tumor (T) and nontumor tissues (NT) from 37 patients with primary HCC was determined as described in the Materials and Methods Section.*

progression since conditional knockout of *JUN* in adult livers reduced the proliferation capacity of hepatocytes after partial hepatectomy, a strong inducer of cell-cycle reentry (26).

However, the exact mechanism by which *JUN* contributes to tumorigenicity remains to be elucidated. *JUN* is located at the end of cellular signaling cascades that include oncogenes that are important for human tumorigenesis (7). The terminal position of *JUN* in cellular signaling pathways make *JUN* a participant in numerous and diverse mechanisms of oncogenesis. In order to fully understand the role of *JUN* in HCC it is therefore important to clarify the network of downstream target genes of *JUN* in HCC. Although our examination did not demonstrate the amplification of *JUN* in primary HCCs, the data presented in this work clearly show *JUN* amplification and overexpression in JHH-2 HCC cells. The JHH-2 cell line therefore provides an efficient tool for analyses of the relationship between *JUN* and oncogenesis.

Acknowledgements

This work was supported by Grants-in-Aid for Scientific Research (20590408) from the Japan Society for the Program of Science (to K.Y.).

References

1 Bosch FX, Ribes J, Cléries R and Díaz M: Epidemiology of hepatocellular carcinoma. Clin Liver Dis *9*: 191-211, 2005.

2 Thorgeirsson SS and Grisham JW: Molecular pathogenesis of human hepatocellular carcinoma. Nat Genet *31*: 339-346, 2002.

3 Inagaki Y, Yasui K, Endo M, Nakajima T, Zen K, Tsuji K, Minami M, Tanaka S, Taniwaki M, Itoh Y, Arii S and Okanoue T: *CREB3L4, INTS3,* and *SNAPAP* are targets for the 1q21 amplicon frequently detected in hepatocellular carcinoma. Cancer Genet Cytogenet *180*: 30-36, 2008.

4 Zen K, Yasui K, Nakajima T, Zen Y, Zen K, Gen Y, Mitsuyoshi H, Minami M, Mitsufuji S, Tanaka S, Itoh Y, Nakanuma Y, Taniwaki M, Arii S, Okanoue T and Yoshikawa T: ERK5 is a target for gene amplification at 17p11 and promotes cell growth in hepatocellular carcinoma by regulating mitotic entry. Genes Chromosomes Cancer *48*: 109-120, 2009.

5 Gen Y, Yasui K, Zen K, Nakajima T, Tsuji K, Endo M, Mitsuyoshi H, Minami M, Itoh Y, Tanaka S, Taniwaki M, Arii S, Okanoue T and Yoshikawa T: A novel amplification target, *ARHGAP5*, promotes cell spreading and migration by negatively regulating RhoA in Huh-7 hepatocellular carcinoma cells. Cancer Lett *275*: 27-34, 2009.

6 Shaulian E and Karin M: AP-1 as a regulator of cell life and death. Nat Cell Biol *4*: E131-136, 2002.

7 Vogt PK: Jun, the oncoprotein. Oncogene *20*: 2365-2377, 2001.

8 Jochum W, Passegué E and Wagner EF: AP-1 in mouse development and tumorigenesis. Oncogene *20*: 2401-2412, 2001.

9 Bohmann D, Bos TJ, Admon A, Nishimura T, Vogt PK and Tjian R: Human proto-oncogene c-*JUN* encodes a DNA-binding protein with structural and functional properties of transcription factor AP-1. Science *238*: 1386-1392, 1987.

10 Maki Y, Bos TJ, Davis C, Starbuck M and Vogt PK: Avian sarcoma virus 17 carries the *Jun* oncogene. Proc Natl Acad Sci USA *84*: 2848-2852, 1987.

11 Schütte J, Minna JD and Birrer MJ: Deregulated expression of human c-*Jun* transforms primary rat embryo cells in cooperation with an activated c-Ha-*ras* gene and transforms rat-1a cells as a single gene. Proc Natl Acad Sci USA *86*: 2257-2261, 1989.

12 Wang ZQ, Liang J, Schellander K, Wagner EF and Grigoriadis AE: c-*Fos*-induced osteosarcoma formation in transgenic mice: cooperativity with c-*Jun* and the role of endogenous c-*Fos*. Cancer Res *55*: 6244-6251, 1995.

13 Mariani O, Brennetot C, Coindre JM, Gruel N, Ganem C, Delattre O, Stern MH and Aurias A: *JUN* oncogene amplification and overexpression block adipocytic differentiation in highly aggressive sarcomas. Cancer Cell *11*: 361-374, 2007.

14 Mathas S, Hinz M, Anagnostopoulos I, Krappmann D, Lietz A, Jundt F, Bommert K, Mechta-Grigoriou F, Stein H, Dörken B and Scheidereit C: Aberrantly expressed c-Jun and JunB are a hallmark of Hodgkin lymphoma cells, stimulate proliferation and synergize with NF-κB. EMBO J *21*: 4104-4113, 2002.

15 Rangatia J, Vangala RK, Singh SM, Peer Zada AA, Elsässer A, Kohlmann A, Haferlach T, Tenen DG, Hiddemann W and Behre G: Elevated c-Jun expression in acute myeloid leukemias inhibits C/EBPα DNA binding *via* leucine zipper domain interaction. Oncogene 22: 4760-4764, 2003.

16 Taniguchi T, Karnan S, Fukui T, Yokoyama T, Tagawa H, Yokoi K, Ueda Y, Mitsudomi T, Horio Y, Hida T, Yatabe Y, Seto M and Sekido Y: Genomic profiling of malignant pleural mesothelioma with array-based comparative genomic hybridization shows frequent non-random chromosomal alteration regions including *JUN* amplification on 1p32. Cancer Sci *98*: 438-446, 2007.

17 Eferl R, Ricci R, Kenner L, Zenz R, David JP, Rath M and Wagner EF: Liver tumor development. c-Jun antagonizes the proapoptotic activity of p53. Cell *112*: 181-192, 2003.

18 Nannya Y, Sanada M, Nakazaki K, Hosoya N, Wang L, Hangaishi A, Kurokawa M, Chiba S, Bailey DK, Kennedy GC and Ogawa S: A robust algorithm for copy number detection using high-density oligonucleotide single nucleotide polymorphism genotyping arrays. Cancer Res *65*: 6071-6079, 2005.

19 Collins C, Rommens JM, Kowbel D, Godfrey T, Tanner M, Hwang SI, Polikoff D, Nonet G, Cochran J, Myambo K, Jay KE, Froula J, Cloutier T, Kuo WL, Yaswen P, Dairkee S, Giovanola J, Hutchinson GB, Isola J, Kallioniemi OP, Palazzolo M, Martin C, Ericsson C, Pinkel D, Albertson D, Li WB and Gray JW: Positional cloning of *ZNF217* and *NABC1*: genes amplified at 20q13.2 and overexpressed in breast carcinoma. Proc Natl Acad Sci USA *95*: 8703-8708, 1998.

20 Fujise K, Nagamori S, Hasumura S, Homma S, Sujino H, Matsuura T, Shimizu K, Niiya M, Kameda H and Fujita K and Ohno T: Integration of hepatitis B virus DNA into cells of six established human hepatocellular carcinoma cell lines. Hepatogastroenterology *37*: 457-460, 1990.

21 Okamoto H, Yasui K, Zhao C, Arii S and Inazawa J: *PTK2* and *EIF3S3* genes may be amplification targets at 8q23-q24 and are associated with large hepatocellular carcinomas. Hepatology *38*: 1242-1249, 2003.

22 Katoh H, Ojima H, Kokubu A, Saito S, Kondo T, Kosuge T, Hosoda F, Imoto I, Inazawa J, Hirohashi S and Shibata T: Genetically distinct and clinically relevant classification of hepatocellular carcinoma: putative therapeutic targets. Gastroenterology *133*: 1475-1486, 2007.

23 Vogt PK and Bader AG: Jun: stealth, stability, and transformation. Mol Cell *19*: 432-433, 2005.

24 Hilberg F, Aguzzi A, Howells N and Wagner EF: c-Jun is essential for normal mouse development and hepatogenesis. Nature *365*: 179-181, 1993.

25 Eferl R, Sibilia M, Hilberg F, Fuchsbichler A, Kufferath I, Guertl B, Zenz R, Wagner EF and Zatloukal K: Functions of c-Jun in liver and heart development. J Cell Biol *145*: 1049-1061, 1999.

26 Behrens A, Sibilia M, David JP, Möhle-Steinlein U, Tronche F, Schütz G and Wagner EF: Impaired postnatal hepatocyte proliferation and liver regeneration in mice lacking c-*Jun* in the liver. EMBO J *21*: 1782-1790, 2002.

Received July 16, 2009
Revised November 3, 2009
Accepted November 5, 2009

Oncogene (2009) 28, 2910–2918

www.nature.com/onc

ORIGINAL ARTICLE

Defective expression of polarity protein PAR-3 gene (*PARD3*) in esophageal squamous cell carcinoma

K Zen[1], K Yasui[1], Y Gen[1], O Dohi[1], N Wakabayashi[1], S Mitsufuji[1], Y Itoh[1], Y Zen[2], Y Nakanuma[2], M Taniwaki[3], T Okanoue[1,4] and T Yoshikawa[1]

[1]*Department of Molecular Gastroenterology and Hepatology, Graduate School of Medical Science, Kyoto Prefectural University of Medicine, Kyoto, Japan;* [2]*Department of Human Pathology, Kanazawa University Graduate School of Medicine, Kanazawa, Japan;* [3]*Department of Molecular Hematology and Oncology, Graduate School of Medical Science, Kyoto Prefectural University of Medicine, Kyoto, Japan and* [4]*Department of Hepatology, Saiseikai Suita Hospital, Suita, Japan*

The partition-defective 3 (PAR-3) protein is implicated in the formation of tight junctions at epithelial cell–cell contacts. We investigated DNA copy number aberrations in human esophageal squamous cell carcinoma (ESCC) cell lines using a high-density oligonucleotide microarray and found a homozygous deletion of *PARD3* (the gene encoding PAR-3). Exogenous expression of *PARD3* in ESCC cells lacking this gene enhanced the recruitment of zonula occludens 1 (ZO-1), a marker of tight junctions, to sites of cell–cell contact. Conversely, knockdown of *PARD3* in ESCC cells expressing this gene caused a disruption of ZO-1 localization at cell–cell borders. A copy number loss of *PARD3* was observed in 15% of primary ESCC cells. Expression of *PARD3* was significantly reduced in primary ESCC tumors compared with their nontumorous counterparts, and this reduced expression was associated with positive lymph node metastasis and poor differentiation. Our results suggest that deletion and reduced expression of *PARD3* may be a novel mechanism that drives the progression of ESCC.
Oncogene (2009) **28,** 2910–2918; doi:10.1038/onc.2009.148; published online 8 June 2009

Keywords: PAR-3; *PARD3*; esophageal squamous cell carcinoma; homozygous deletion; tight junction; metastasis

Introduction

Esophageal cancer is the sixth leading cause of cancer mortality worldwide (Enzinger and Mayer, 2003). Of the two main histological subtypes of esophageal cancer, squamous cell carcinoma is prevalent worldwide, although the incidence of adenocarcinoma has been increasing in North America and Europe (Vizcaino *et al.*, 2002).

Correspondence: Dr K Yasui, Department of Molecular Gastroenterology and Hepatology, Graduate School of Medical Science, Kyoto Prefectural University of Medicine, 465 Kajii-cho, Kamigyo-ku, Kyoto 602-8566, Japan.
E-mail: yasuik@koto.kpu-m.ac.jp
Received 9 December 2008; revised 13 April 2009; accepted 7 May 2009; published online 8 June 2009

Inactivation of tumor suppressor genes is critical to the development and progression of human malignancies. Much effort has been put into finding homozygous deletions in cancer cells in the expectation that they harbor tumor suppressor genes. Suppressor genes that have been identified partly from homozygous deletions include *CDKN2A* (Kamb *et al.*, 1994), *PTEN* (Li *et al.*, 1997) and *SMAD4* (Hahn *et al.*, 1996). The recent introduction of high-density oligonucleotide microarrays designed for typing of single nucleotide polymorphisms (SNPs) facilitates high-resolution mapping of chromosomal amplifications, deletions and losses of heterozygosity (Mei *et al.*, 2000; Zhao *et al.*, 2004).

Cell polarization and the formation of cell–cell junctions are coupled processes that are essential to tissue morphogenesis (Macara, 2004). Loss of cell–cell adhesion and cell polarity is commonly observed in advanced tumors and correlates strongly with their invasion into adjacent tissues and the formation of metastases (Wodarz and Näthke, 2007).

It has become apparent that polarity is largely regulated by a conserved set of proteins referred to as partition-defective (PAR) proteins (Kemphues *et al.*, 1988; Macara, 2004; Suzuki and Ohno, 2006). These proteins were first identified in the zygote of *Caenorhabditis elegans*, where they specify the anterior–posterior body axis. They are also essential for asymmetric cell division in *Drosophila melanogaster*. The mammalian homologs of the *C. elegans* polarity proteins have evolutionarily conserved functions in the establishment of cell polarity in various cell types. One of these homologs, PAR-3, contains one self-oligomerization domain in the N terminus, three PDZ protein interaction domains and one atypical protein kinase C (aPKC)-binding domain (Izumi *et al.*, 1998; Joberty *et al.*, 2000; Lin *et al.*, 2000; Assémat *et al.*, 2008). These domains enable PAR-3 to form a conserved protein complex with PAR-6 and aPKC (Macara, 2004; Suzuki and Ohno, 2006). In mammalian epithelial cells, this PAR-3–PAR-6–aPKC complex assembles at tight junctions, where it is necessary for the establishment of apico-basal polarity.

Thus, deletion of PAR protein genes in tumor cells may disrupt cell polarity and adhesion. To identify the

genes that are potentially involved in human esophageal squamous cell carcinoma (ESCC), we investigated DNA copy number aberrations in ESCC cell lines using high-resolution SNP arrays. We show that the gene encoding human PAR-3 protein, *PARD3*, is homozygously deleted in ESCC cells, and that this deletion affects the formation of tight junctions in these cells. Furthermore, we show that reduced expression of *PARD3* is associated with the aggressiveness of primary ESCC tumors.

Results

Identification of homozygous deletion of PARD3

To identify genes potentially involved in ESCC, we screened for DNA copy number aberrations in 20 ESCC cell lines by Affymetrix GeneChip Mapping 250K array analysis. Of the 20 cell lines screened, KYSE30 and KYSE270 cells exhibited homozygous deletions at the chromosomal region 10p11 (Figure 1a). The estimated extent of the common region of deletion was ~280 kb between the markers SNP_A-2051960 and SNP_A-1867256, which includes a single gene *PARD3* (Supplementary Figure S1). The extent of the shortest region of overlap of homozygous deletions was narrowed down to exons 3–22 of *PARD3* by genomic PCR analyses (Figures 1b and c).

Copy number and expression of PARD3 *in ESCC cell lines*

We analysed the DNA copy number and expression level of *PARD3* in 20 ESCC cell lines and normal lymphocytes and in esophageal epithelial cells as a control (Figure 2). Comparison with normal esophageal epithelial cells showed lower expression of *PARD3* in 18 of the 20 ESCC cell lines (Figure 2b). The absence of the *PARD3* gene in the KYSE30 and KYSE270 cell lines was confirmed by real-time quantitative reverse transcription (RT)–PCR and immunoblot analyses. These assays did not detect the expression of *PARD3* mRNA and the PAR-3 protein, respectively (Figures 2b and c). Analyses of the cell lines by real-time quantitative RT–PCR and immunoblot indicated varying expression levels of *PARD3* mRNA, and three forms of the PAR-3 protein with molecular weights of 180, 150 and 100 kDa, respectively (Figures 2b and c).

PAR-3-dependent recruitment of ZO-1 to sites of cell–cell contact in ESCC cells

To determine whether the deletion of *PARD3* leads to defective tight junction formation in ESCC cells, we determined the effect of *PARD3* deletion on the subcellular localization of zonula occludens 1 (ZO-1), a marker of cellular tight junctions (Stevenson *et al.*, 1986). For this purpose, we compared the colocalization

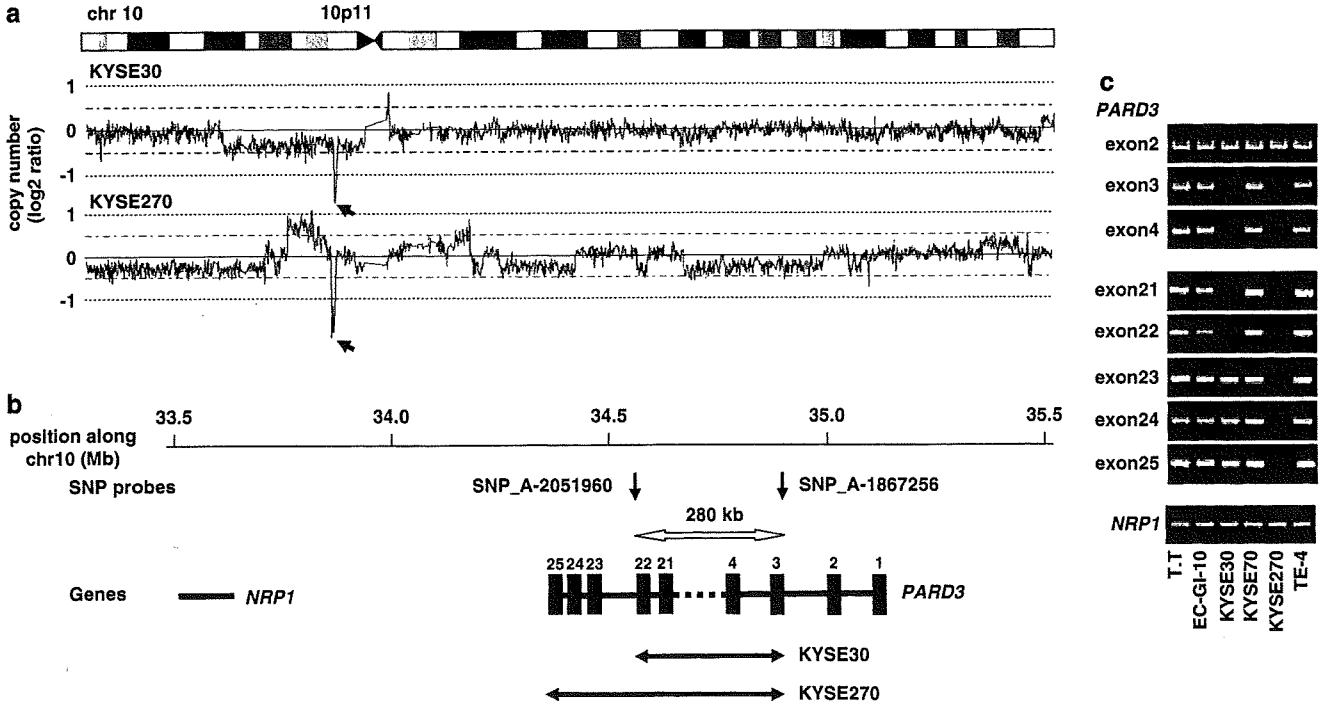

Figure 1 Homozygous deletion of *PARD3* in ESCC cell lines. (**a**) Chromosome 10 cytoband map and copy numbers determined by Affymetrix GeneChip Mapping 250K arrays of KYSE30 and KYSE270 cells. Arrows indicate the loci for homozygous deletions at position 10p11. (**b**) Map of 10p11 encompassing the region that is homozygously deleted in KYSE30 and KYSE270 cells. The position of the Affymetrix SNP probes, the two genes (*NRP1* and *PARD3*) and the exons of *PARD3* is shown according to the UCSC genome database 2006 (http://genome.ucsc.edu/). Horizontal arrows indicate the regions homozygously deleted in KYSE30 and KYSE270 cells as determined by genomic PCR analyses (see panel c). The horizontal white closed arrow indicates the minimal common region of deletion. (**c**) PCR analysis of each exon of the *PARD3* and *NRP1* genes using a genomic DNA template derived from six ESCC cell lines.

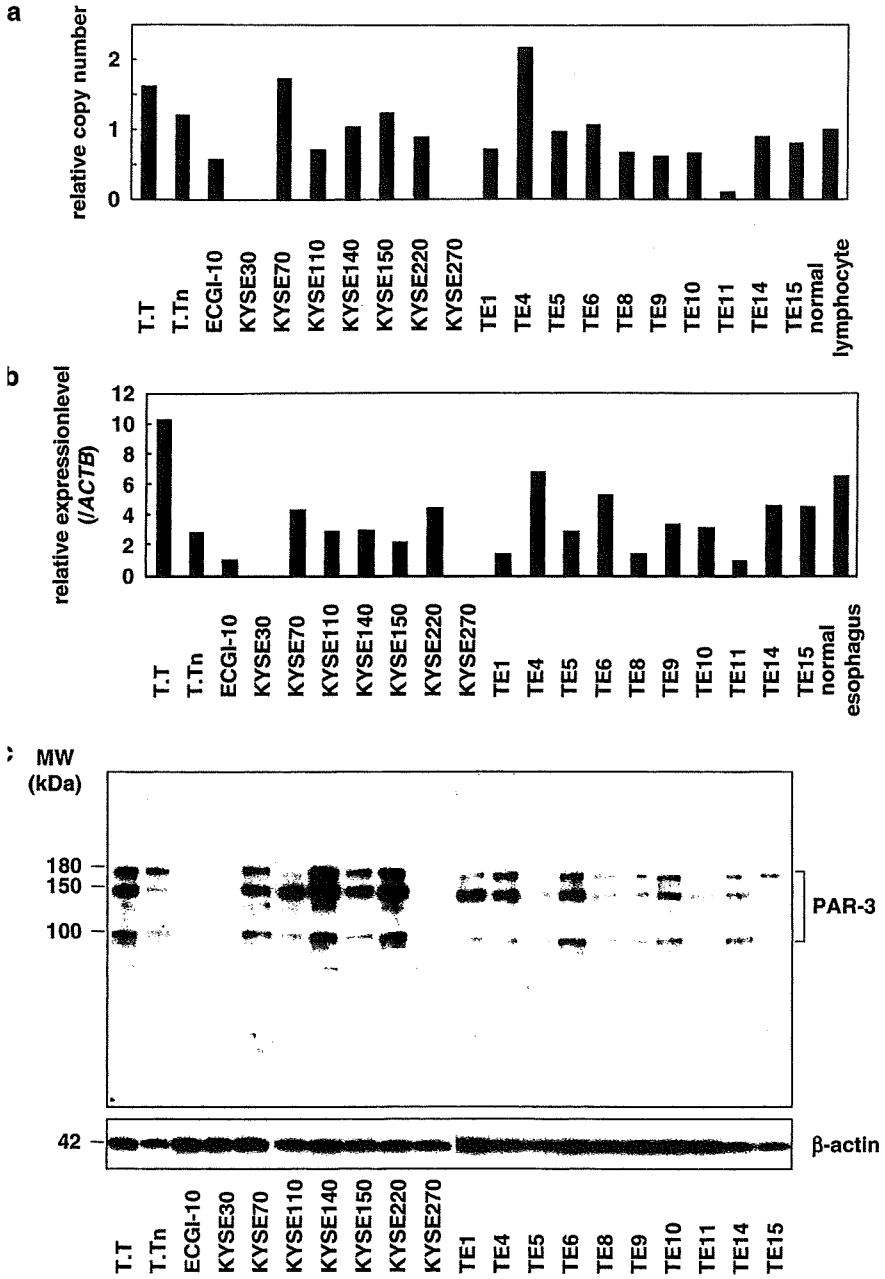

Figure 2 Copy number and expression level of *PARD3* in 20 ESCC cell lines. (**a**) The copy number of *PARD3* in 20 ESCC cell lines as measured by real-time quantitative PCR with reference to the LINE-1 control. Values are normalized such that the copy number in genomic DNA derived from normal lymphocytes has a value of 1. (**b**) Relative expression levels of *PARD3* in 20 ESCC cell lines and normal esophagus as evaluated by real-time quantitative reverse transcription (RT)–PCR. The results are presented as the expression level of each gene relative to a reference gene (*ACTB*) in order to correct for variations in the amount of RNA. (**c**) Immunoblot analyses of protein levels of PAR-3 in the indicated cell lines. β-Actin was used as an internal control.

of PAR-3 and ZO-1 by immunofluorescence in two *PARD3*-expressing cell lines (T.T and TE-4) with that in two cell lines lacking *PARD3* (KYSE30 and KYSE270). ZO-1 colocalized with PAR-3 at sites of cell–cell contact in T.T and TE-4 cells (Figure 3a). In contrast, ZO-1 was only weakly observed at sites of cell–cell contact in KYSE30 cells and was barely detected in KYSE270 cells (Figure 3a), despite the fact that the ZO-1 protein could be detected by immunoblotting in all cell lines (Figure 3b). As expected, the expression of PAR-3 was not detected in KYSE30 or KYSE270 cells (Figure 3a).

To further confirm that the absence of PAR-3 was the cause of the aberrant localization of ZO-1 in the KYSE30 and KYSE270 cells, we determined whether transfection of *PARD3* into these cells could restore ZO-1 localization to tight junctions. After transfection, the expression of PAR-3 (molecular weight, 180 kDa) in the *PARD3*-transfected KYSE30 and KYSE270 cells was detected by immunoblotting analysis (Figure 4a).

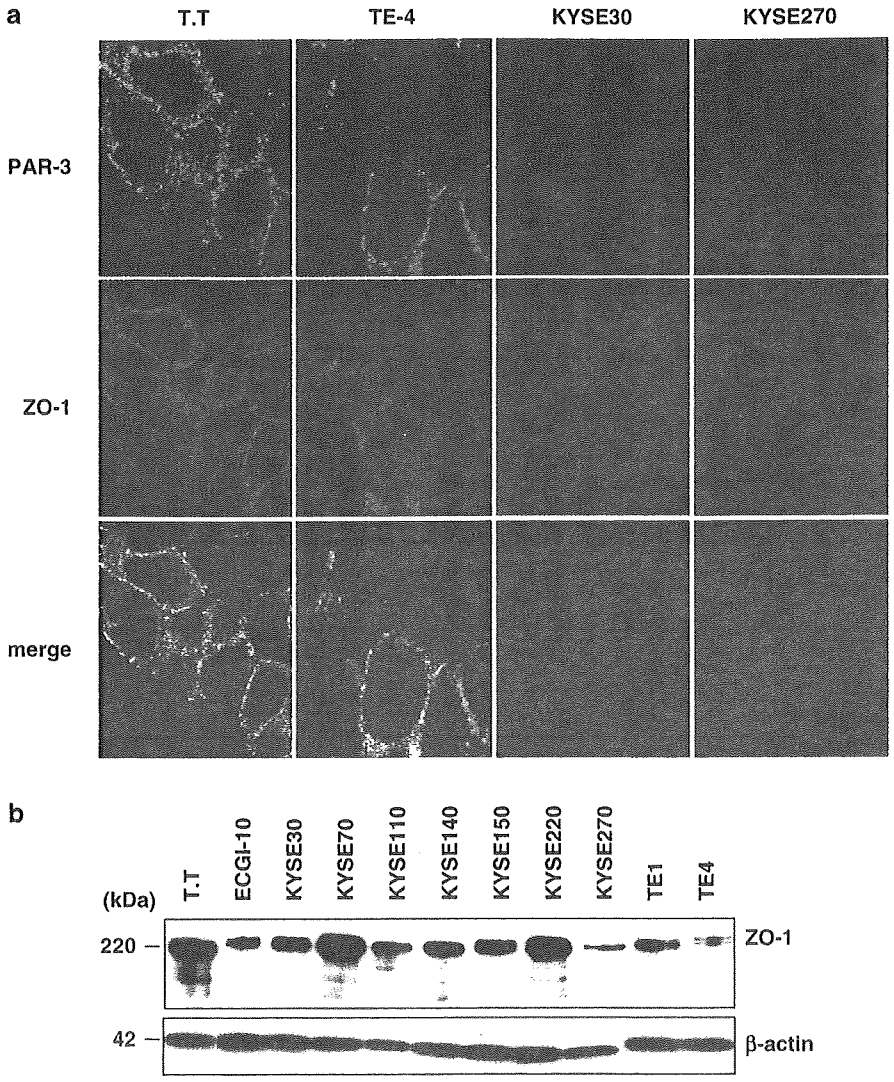

Figure 3 Effect of *PARD3* deletion on the subcellular localization of ZO-1. (**a**) Subcellular localization of PAR-3 and ZO-1 in PAR-3-expressing (T.T, TE-4) and non-expressing (KYSE30, KYSE270) cells. The cells were doubly stained with anti-PAR-3 (green) and anti-ZO-1 (red), and were viewed with a confocal laser scanning microscope. PAR-3 and ZO-1 colocalized at cell–cell borders in the T.T and TE-4 cells. The nuclear staining observed with anti-PAR-3 in the KYSE30 and KYSE270 cells is probably nonspecific because of the absence of *PARD3*. Original magnifications, × 1000. (**b**) Immunoblotting analyses of ZO-1 and β-actin, used as an internal control, in 11 ESCC cell lines.

Immunocytochemistry showed that, in addition to a diffuse staining, PAR-3 could now be detected in a linear manner at cell–cell borders in the *PARD3*-transfected KYSE30 and KYSE270 cells, in which it colocalized with ZO-1 (Figure 4b). Transfection of *PARD3* led to a stronger staining of ZO-1 at sites of cell–cell contact compared with control-transfected cells (Figure 4b). This was despite the fact that the total level of ZO-1 was the same in *PARD3* and control transfectants (Figure 4c). Knockdown of the *PARD3* expression in T.T cells was carried out using RNA interference (RNAi). After treatment of T.T cells with small interfering RNA (siRNA) targeting *PARD3*, we observed a decrease in the PAR-3 protein level relative to that observed for cells receiving negative control siRNA, transfection agent alone or left untreated (Figure 4a). Suppression of the PAR-3 expression by siRNA caused a disruption of localization of ZO-1 at cell–cell borders (Figure 4b), although the total level of ZO-1 was unchanged (Figure 4c). Taken together, these findings suggest that PAR-3 promotes the recruitment of ZO-1 to sites of cell–cell contact.

PAR-3 and cell migration

To investigate the role of PAR-3 in cell motility, we performed a monolayer wound-healing assay in knockdown T.T cells. Knockdown of the *PARD3* expression was conducted as described above. Wound closure was shown to be unchanged among *PARD3* siRNA-treated cells, negative control siRNA-treated cells and untreated cells (Supplementary Figure S2).

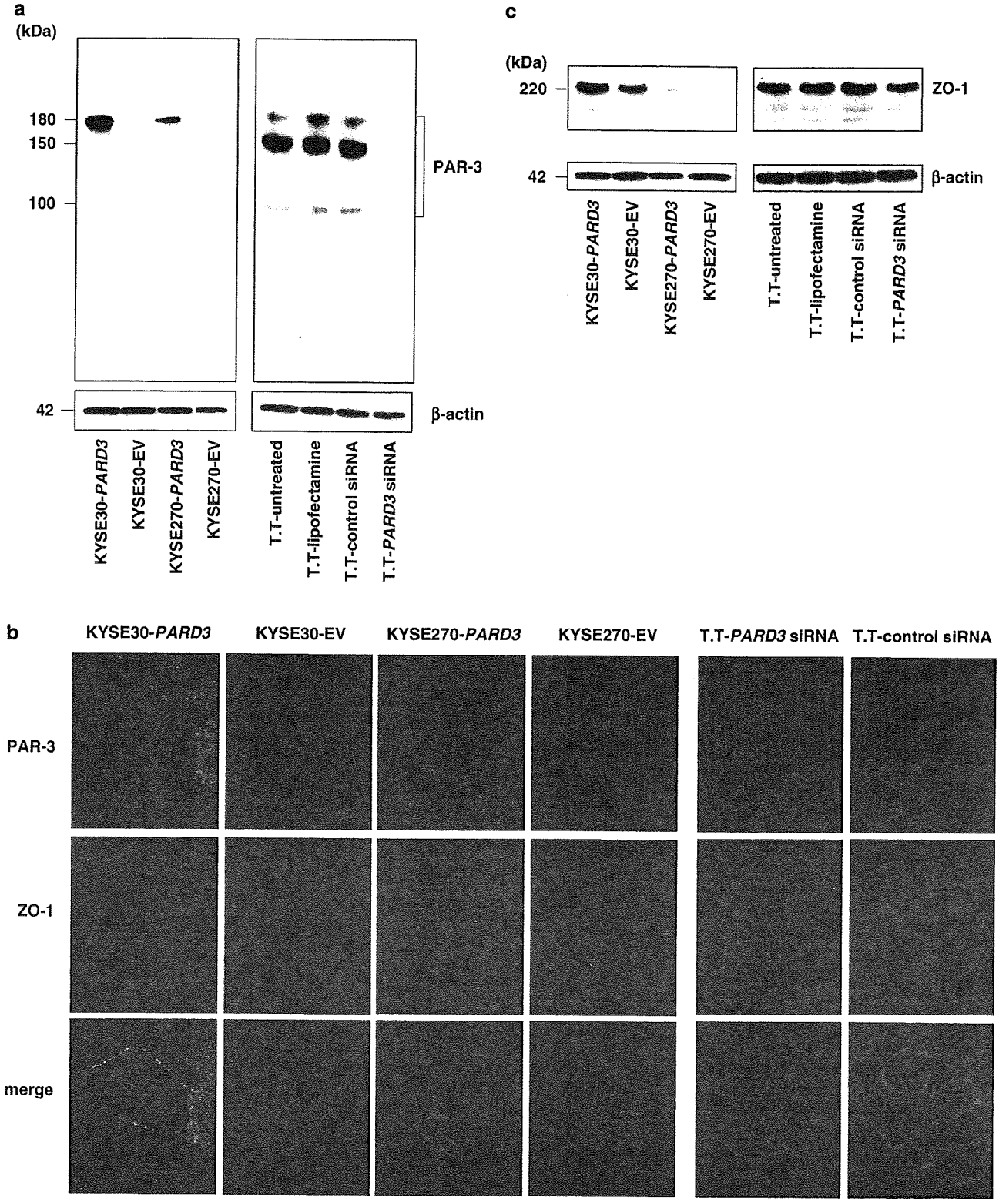

Figure 4 Effect of enforced expression of *PARD3* or knockdown of *PARD3* expression on the subcellular localization of ZO-1. KYSE30 and KYSE270 cells were transfected with the *PARD3* expression vector or with an empty vector (EV). T.T cells were treated with siRNA targeting *PARD3*, control siRNA, transfection agent (lipofectamine) alone or left untreated. (**a**) Immunoblot analysis of PAR-3. Analysis of β-actin served as an internal control. (**b**) Subcellular localization of PAR-3 and ZO-1 in transiently transfected cells. The cells were doubly stained with anti-PAR-3 (green) and anti-ZO-1 (red), and were viewed with a confocal laser scanning microscope. Original magnification, × 1000. (**c**) Immunoblot analyses of ZO-1 and an internal control, β-actin.

This suggests that the suppression of PAR-3 may not affect cell migration.

Analysis of PARD3 *defects in primary tumors*

To determine whether the loss of *PARD3* observed in KYSE30 and KYSE270 carcinoma cell lines was relevant to primary carcinomas in humans, we first determined the DNA copy number of *PARD3* in 40 primary ESCC tumors (Figure 5a). For this analysis, the values were normalized such that the copy number in genomic DNA derived from normal lymphocytes was given a value of 1. Copy number changes were counted as losses if the results of the analysis for a given ESCC tumor were <0.7 (Berggren *et al.*, 2003). Using these parameters, a copy number loss of *PARD3* was observed in 6 (15%) of the 40 tumors.

We then further quantified the mRNA levels of *PARD3* in the available paired tumor and nontumor tissues from 33 ESCC patients (Figure 5b). Patient and tumor characteristics are summarized in Supplementary Table S2. The expression of *PARD3* mRNA was significantly reduced in 23 (70%) of the 33 tumors when compared with their nontumorous tissue counterparts (Wilcoxon signed-rank test, $P=0.017$). To clarify the relationship between the expression level of *PARD3* and various clinicopathological parameters, we correlated the *PARD3* expression level with clinical data that was available for 28 of the patients. For this purpose, tumors were divided into one of two groups based on reduction in *PARD3* levels: tumor tissue (T) <nontumor tissue (NT), or not reduced (T⩾NT). Reduced expression of *PARD3* was significantly associated with a younger age (⩽65 years), positive lymph node metastasis and poor differentiation (Table 1). These findings suggest that reduced expression of *PARD3* is important not only for cancer cell lines but also for the tumorigenic properties of primary tumors.

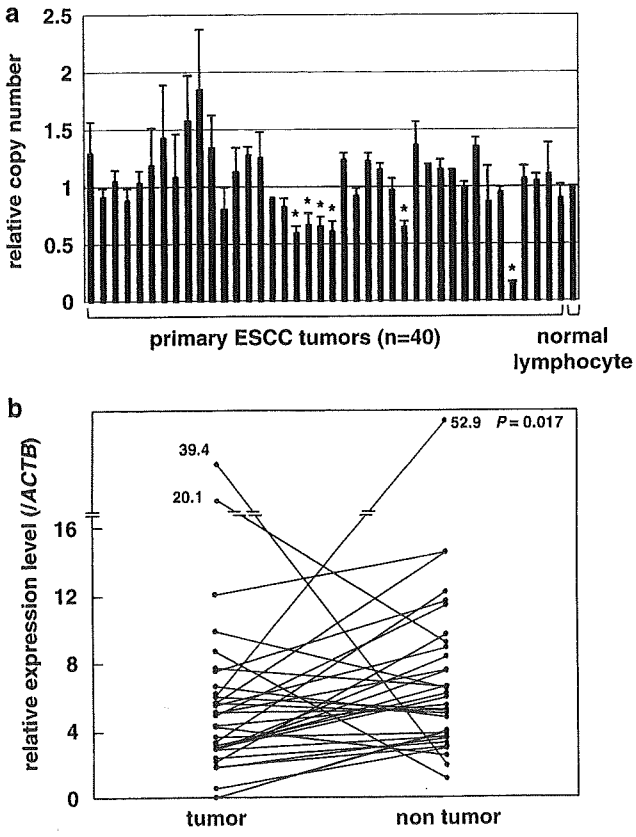

Figure 5 Copy number and expression level of *PARD3* in primary ESCC tumors. (**a**) The copy number of *PARD3* in each of 40 primary ESCC tumors was determined as described in Figure 2a. Values are represented as the mean ± s.d. of three independent experiments. Asterisks indicate tumors with a loss (<0.7) of *PARD3*. The copy number of normal lymphocytes served as a control. (**b**) The relative expression of *PARD3* in paired tumor (T) and nontumor tissues (NT) from 33 patients with primary ESCCs was determined as described in Figure 2b. *P*-values of <0.05 were considered significant.

Discussion

Homozygous deletions have been useful in the positional cloning of a number of tumor suppressor

Table 1 Relationship between clinicopathological features and levels of expression of *PARD3* in 28 primary ESCCs

Characteristics	*PARD3*		P-*value*[a]
	T<NT (n=*18*)	*T⩾NT* (n=*10*)	
Age (years)			
⩽65	11	2	0.037
>65	7	8	
Gender			
Male	14	8	0.891
Female	4	2	
Tumor diameter (cm)			
⩽3 cm	6	7	0.062
>3 cm	12	3	
Stage			
I/II	8	7	0.194
III/IV	10	3	
T classification			
T1/T2	8	7	0.194
T3/T4	10	3	
N status			
N0	5	7	0.031
N1	13	3	
M status			
M0	15	10	0.172
M1	3	0	
Histological differentiation			
Well/moderate	11	10	0.023
Poor	7	0	

Abbreviations: ESCC, esophageal squamous cell carcinoma; NT, nontumor tissue; T, tumor tissue.
[a]χ^2-Test.

genes (Friend *et al.*, 1986; Kamb *et al.*, 1994; Hahn *et al.*, 1996; Li *et al.*, 1997). A putative tumor suppressor is believed to lie on the chromosomal region 10p in ESCC (Aoki *et al.*, 1994). In this study, using high-density SNP arrays, we identified a novel homozygous deletion at the chromosomal region 10p11 in 2 out of 20 ESCC cell lines. Subsequent detailed analyses narrowed down the extent of the shortest region of overlap of the homozygous deletions to exons 3–22 of the gene *PARD3*. Recently, homozygous deletion of *PARD3* has been reported in two lung cancer cell lines (Nagayama *et al.*, 2007).

A few studies have suggested an association of *PARD3* with tumors (Fang and Xu, 2001; Zitzelsberger *et al.*, 2004), and *PARD3* was reported to be amplified in radiation-transformed neoplastic retinal pigment epithelial cell lines (Zitzelsberger *et al.*, 2004). Also, various splicing transcripts of *PARD3* are expressed in primary hepatocellular carcinomas, and the expression of exon 17b deleted *PARD3* variants is downregulated in these carcinomas compared with the surrounding nontumorous liver tissues (Fang and Xu, 2001). However, the biological function of *PARD3* and its clinical significance for cancer are poorly understood. In this study, a gain of *PARD3* copy number (defined as twice the level of normal DNA) was observed in only 1 of the 20 ESCC cell lines tested (TE4 cells) and in none of the 40 primary ESCC tumors analysed. Conversely, a loss of *PARD3* was detected in 15% of the primary ESCC tumors examined, and a reduced expression of *PARD3* mRNA was found in primary ESCC tumors compared with their nontumorous counterparts. The reduced expression of *PARD3* was associated with aggressive ESCC phenotypes, such as positive lymph node metastasis and poor differentiation. To validate these results at the protein level, we unsuccessfully tried to carry out the immunohistochemical analysis of PAR-3 on formalin-fixed and paraffin-embedded sections of primary ESCC specimens. We assume that the anti-PAR-3 antibody is not suitable for formalin-fixed and paraffin-embedded sections. Further studies in more numerous primary samples and studies using immunohistochemistry are needed to determine the clinical importance of PAR-3 in ESCC.

PAR-3 has been implicated in the formation of normal tight junctions at epithelial cell–cell contacts (Joberty *et al.*, 2000; Macara, 2004; Chen and Macara, 2005; Suzuki and Ohno, 2006). PAR-3 plays the role of a scaffold in the recruitment of proteins, such as PAR-6 or aPKC, that are involved in the formation of these junctions (Assémat *et al*, 2008). In agreement with these data, our immunocytochemical analyses showed that PAR-3 colocalized with the tight junction component, ZO-1, at sites of cell–cell contact in T.T and TE-4 cells that express *PARD3*. Unexpectedly, ZO-1 was weakly detected at sites of cell–cell contact in KYSE30 cells that lack *PARD3*. On the other hand, ZO-1 was barely detected in KYSE270 cells, which also lack *PARD3*. Exogenous expression of *PARD3* resulted in the recruitment of ZO-1 to sites of cell–cell contact in KYSE30 and KYSE270 cells without affecting the expression level of ZO-1. Conversely, knockdown of *PARD3* in T.T cells that express this gene caused a disruption of localization of ZO-1 at cell-cell borders. Taken together, these findings suggest that PAR-3 promotes the recruitment of ZO-1 to sites of cell–cell contact, although it may not always be essential for this localization of ZO-1. The finding that *PARD3* affects the formation of tight junction in ESCC cells might partially explain the observed association between the reduced expression of *PARD3* and positive lymph node metastasis, and between poor differentiation of primary ESCCs. However, our wound-healing assay did not show any effect of PAR-3 on cell migration. Further functional studies are needed to determine the implication of PAR-3 in ESCC invasion and metastasis.

Our finding that PAR-3 is important, but not essential, for tight junction formation and ZO-1 recruitment are in partial agreement with previous observations. The targeted disruption of the mouse PAR-3 gene (*Pard3*) results in embryonic lethality with defective epicardial development (Hirose *et al.*, 2006). *Pard3*-deficient epicardial progenitor cells do not form epicardial cysts from which the epicardium is derived. These cells show defects in the localization of PAR-6 and aPKC to the apical domain, but a normal localization of ZO-1 to cell–cell junctions. Interestingly, not all epithelial cells are affected in the *Pard3*-deficient embryo, which may be due to the proposed functional redundancy of PAR-3 and the PAR-3-related protein PAR-3L/PAR-3β (Gao *et al.*, 2002; Kohjima *et al.*, 2002). The function of PAR-3 has also been examined in MDCK II canine epithelial cells (Chen and Macara, 2005). In that study, withdrawal of calcium from the medium caused rapid loss of cell–cell junctions, which could be reversed by the re-addition of calcium (a calcium switch experiment). The normal relocalization of tight junction components at cell–cell contacts within 30 min after re-addition of calcium was profoundly delayed in cells lacking PAR-3, although tight junctions could eventually form even without re-expression of PAR-3.

The exact mechanism by which PAR-3 modulates tight junctions and contributes to tumorigenicity remains to be elucidated. Besides PAR-6 and aPKC, PAR-3 also interacts with other proteins such as 14-3-3, LIMK2 and the Rac-specific guanine nucleotide exchange factor STEF/Tiam1 (Humbert *et al.*, 2006; Assémat *et al.*, 2008). Moreover, recent studies have shown that the PAR-3–PAR-6–aPKC complex associates with the tumor suppressor VHL (von Hippel–Lindau protein) or with PTEN (phosphatase and tensin homologue deleted on chromosome ten) (Wodarz and Näthke, 2007), suggesting potential mechanisms by which PAR-3 might modulate tumorigenicity. Although the mechanism of PAR-3 function in tumors remains to be elucidated and the findings must be verified in a larger sample number, the data presented in this work clearly suggest a role for PAR-3 deletion in the tumorigenesis of ESCC.

Materials and methods

Cell lines and primary tumors
The ESCC cell lines TE-1, TE-5, TE-9, TE-15 and EC-GI-10 were obtained from RIKEN Bioresource Center (Tsukuba, Japan); T.T, T.Tn, KYSE30, KYSE70, KYSE110, KYSE140, KYSE150, KYSE220 and KYSE270 were from Japan Health Sciences Foundation (Osaka, Japan); and TE-4, TE-6, TE-8, TE-10, TE-11 and TE-14 were from Cell Resource Center for Biomedical Research, Tohoku University (Sendai, Japan). All cell lines were maintained in Dulbecco's modified Eagle's medium supplemented with 10% fetal bovine serum. Genomic DNA was isolated from the cell lines with the DNeasy Mini Kit (Qiagen, Tokyo, Japan).

Paired tumor and nontumor tissues were obtained during upper gastrointestinal endoscopic inspection from 40 ESCC patients who underwent biopsy for diagnostic purposes at the Hospital of Kyoto Prefectural University of Medicine (Kyoto, Japan). All biopsy specimens were immediately frozen in liquid nitrogen and stored at −80 °C until required. Genomic DNA and total RNA were isolated from primary samples with the AllPrep DNA/RNA Mini Kit (Qiagen). All tumor samples were available for DNA analyses, and 33 paired tumor and nontumor samples were available for mRNA analyses. Before the study, informed consent was obtained and the study was approved by ethics committees.

Array analysis
Array analyses were carried out with the GeneChip Mapping 250K Sty array (Affymetrix, Santa Clara, CA, USA) according to the manufacturer's instructions. In brief, 250 ng of genomic DNA was digested with a restriction enzyme (*Sty*I), ligated to an adaptor and amplified by PCR. Amplified products were fragmented, labeled by biotinylation and hybridized to the microarrays. Hybridization was detected by incubation with streptavidin–phycoerythrin conjugates, followed by scanning of the array, and analysis was carried out as described earlier (Kennedy *et al.*, 2003). Copy number changes were calculated using the Copy Number Analyzer for Affymetrix GeneChip Mapping Arrays (CNAG; http://www.genome.umin.jp; Nannya *et al.*, 2005).

PCR analysis
Conventional PCR was performed using Ex Taq DNA Polymerase (Takara, Otsu, Japan) as described by the manufacturer. Genomic DNA and mRNA were quantified with a real-time fluorescence detection method as described earlier (Inagaki *et al.*, 2008). Total RNA derived from normal human esophageal epithelial cells was purchased from Ambion (Austin, TX, USA). Single-stranded cDNAs were generated from total RNAs using QuantiTect Reverse Transcription Kit (Qiagen). Primers used for genomic PCR and RT–PCR are listed in Supplementary Table S1. Endogenous controls for mRNA and genomic DNA levels were *ACTB* and the long interspersed nuclear element 1 (LINE-1) (Zhao *et al.*, 2004), respectively.

Immunoblotting
Immunoblots were prepared according to the previously reported methods (Yasui *et al.*, 2001). Cell lysates (20 μg protein per sample) were separated by SDS–polyacrylamide gel electrophoresis using 10% acrylamide gels. The anti-PAR-3 polyclonal antibody was obtained from Upstate Biotechnology (Lake Placid, NY, USA), the anti-β-actin monoclonal antibody from Sigma-Aldrich (Tokyo, Japan) and the anti-ZO-1 monoclonal antibody from Zymed (South San Francisco, CA, USA). The anti-PAR-3, anti-ZO-1 and anti-β-actin antibodies were used for immunoblotting at dilutions of 1:500, 1:250 and 1:5000, respectively. For secondary immunodetection, anti-rabbit or anti-mouse immunoglobulin (Ig) (Amersham, Tokyo, Japan) was diluted 1:5000. Protein binding was detected using the ECL system (Amersham).

Transient expression of PARD3
The full-length human *PARD3* cDNA (clone ID: IOH62499) was obtained from Invitrogen (Carlsbad, CA, USA) and was subcloned into pcDNA3.2/V5-DEST vector (Invitrogen) to generate a mammalian expression vector. The *PARD3* expression vector, or an empty vector, was transfected into KYSE30 and KYSE270 cells using the Effectene Transfection Reagent Kit (Qiagen) according to the manufacturer's instructions. After 48 h incubation, the cell lysates were analysed by immunoblotting for detection of the expression of PAR-3 protein.

RNAi
Small interfering RNA duplex oligoribonucleotides targeting *PARD3* (5′-AAUGAUGGGUGUACGCAUGGCUUGG-3′) and control (non-silencing) siRNA duplexes were synthesized by Invitrogen in order to investigate the role of PAR-3 in ZO-1 localization and cell motility. The siRNAs were delivered into T.T cells using Lipofectamine RNAiMAX (Invitrogen), according to the manufacturer's protocol.

Immunofluorescence microscopy
KYSE30 and KYSE270 cells were transfected with the *PARD3* expression vector or the empty vector. T.T cells were transfected with either siRNA targeting *PARD3* or negative control siRNA. After 24 h incubation, the cells were collected, reseeded on glass slides and incubated overnight. The cells were fixed with 3.7% formaldehyde, permeabilized with 0.2% Triton X-100 and incubated with phosphate-buffered saline containing 1% bovine serum albumin. The cells were then treated with a mixture of anti-PAR-3 and anti-ZO-1 antibodies at a dilution of 1:500 and 1:100, respectively, for 1 h at 37 °C. The second antibodies used were a mixture of fluorescein isothiocyanate-conjugated anti-rabbit Ig (Cappel, Aurora, OH, USA) and rhodamine-conjugated anti-mouse Ig (Cappel) for the detection of PAR-3 and ZO-1, respectively. Samples were examined using a confocal laser scanning microscope (SV1000; Olympus, Tokyo, Japan).

Monolayer wound healing assay
T.T cells were transfected with either siRNA targeting *PARD3* or negative control siRNA, or left untreated. After 24 h, cells in Dulbecco's modified Eagle's medium with 1% fetal bovine serum were seeded on glass slides and allowed to adhere overnight. Wounds were scratched into the cell monolayer using a sterile 200-μl pipette tip, rinsed the cells with phosphate-buffered saline and added Dulbecco's modified Eagle's medium containing 10% fetal bovine serum with mitomycin C (0.5 μg/ml, Nacalai Tesque, Kyoto, Japan). Mitomycin C blocks mitosis and thus allows analysis of cell migration in the absence of cell proliferation. Cells were allowed to migrate into the wound over a period of 24 h before fixation. Wound widths were measured in three randomly selected regions at 0, 12 and 24 h after wounding. Cells were stained with Giemsa stain (Nacalai Tesque, Kyoto, Japan). Experiments were repeated at least three times.

Statistical analysis
Statistical analyses were carried out using SPSS 15.0 software (SPSS, Chicago, IL, USA). χ^2 or Wilcoxon signed-rank test was used. *P*-values of <0.05 were considered significant.

Conflict of interest

The authors declare no conflict of interest.

Acknowledgements

This study was supported by Grants-in-Aid for Scientific Research (18390223 and 20590408) from the Japan Society for the Program of Science (KY).

References

Aoki T, Mori T, Du X, Nisihira T, Matsubara T, Nakamura Y. (1994). Allelotype study of esophageal carcinoma. *Genes Chromosomes Cancer* **10**: 177–182.

Assémat E, Bazellières E, Pallesi-Pocachard E, Le Bivic A, Massey-Harroche D. (2008). Polarity complex proteins. *Biochim Biophys Acta* **1778**: 614–630.

Berggren P, Kumar R, Sakano S, Hemminki L, Wada T, Steineck G *et al.* (2003). Detecting homozygous deletions in the CDKN2A (p16(INK4a))/ARF(p14(ARF)) gene in urinary bladder cancer using real-time quantitative PCR. *Clin Cancer Res* **9**: 235–242.

Chen X, Macara IG. (2005). Par-3 controls tight junction assembly through the Rac exchange factor Tiam1. *Nat Cell Biol* **7**: 262–269.

Enzinger PC, Mayer RJ. (2003). Esophageal cancer. *N Engl J Med* **349**: 2241–2252.

Fang CM, Xu YH. (2001). Down-regulated expression of atypical PKC-binding domain deleted asip isoforms in human hepatocellular carcinomas. *Cell Res* **11**: 223–229.

Friend SH, Bernards R, Rogelj S, Weinberg RA, Rapaport JM, Albert DM *et al.* (1986). A human DNA segment with properties of the gene that predisposes to retinoblastoma and osteosarcoma. *Nature* **323**: 643–646.

Gao L, Macara IG, Joberty G. (2002). Multiple splice variants of Par3 and of a novel related gene, Par3L, produce proteins with different binding properties. *Gene* **294**: 99–107.

Hahn SA, Schutte M, Hoque AT, Moskaluk CA, da Costa LT, Rozenblum E *et al.* (1996). DPC4, a candidate tumor suppressor gene at human chromosome 18q21.1. *Science* **271**: 350–353.

Hirose T, Karasawa M, Sugitani Y, Fujisawa M, Akimoto K, Ohno S *et al.* (2006). PAR3 is essential for cyst-mediated epicardial development by establishing apical cortical domains. *Development* **133**: 1389–1398.

Humbert PO, Dow LE, Russell SM. (2006). The Scribble and Par complexes in polarity and migration: friends or foes? *Trends Cell Biol* **16**: 622–630.

Inagaki Y, Yasui K, Endo M, Nakajima T, Zen K, Tsuji K *et al.* (2008). CREB3L4, INTS3, and SNAPAP are targets for the 1q21 amplicon frequently detected in hepatocellular carcinoma. *Cancer Genet Cytogenet* **180**: 30–36.

Izumi Y, Hirose T, Tamai Y, Hirai S, Nagashima Y, Fujimoto T *et al.* (1998). An atypical PKC directly associates and colocalizes at the epithelial tight junction with ASIP, a mammalian homologue of *Caenorhabditis elegans* polarity protein PAR-3. *J Cell Biol* **143**: 95–106.

Joberty G, Petersen C, Gao L, Macara IG. (2000). The cell-polarity protein Par6 links Par3 and atypical protein kinase C to Cdc42. *Nat Cell Biol* **2**: 531–539.

Kamb A, Gruis NA, Weaver-Feldhaus J, Liu Q, Harshman K, Tavtigian SV *et al.* (1994). A cell cycle regulator potentially involved in genesis of many tumor types. *Science* **264**: 436–440.

Kemphues KJ, Priess JR, Morton DG, Cheng NS. (1988). Identification of genes required for cytoplasmic localization in early *C. elegans* embryos. *Cell* **52**: 311–320.

Kennedy GC, Matsuzaki H, Dong S, Liu WM, Huang J, Liu G *et al.* (2003). Large-scale genotyping of complex DNA. *Nat Biotechnol* **21**: 1233–1237.

Kohjima M, Noda Y, Takeya R, Saito N, Takeuchi K, Sumimoto H. (2002). PAR3beta, a novel homologue of the cell polarity protein PAR3, localizes to tight junctions. *Biochem Biophys Res Commun* **299**: 641–646.

Li J, Yen C, Liaw D, Podsypanina K, Bose S, Wang SI *et al.* (1997). PTEN, a putative protein tyrosine phosphatase gene mutated in human brain, breast, and prostate cancer. *Science* **275**: 1943–1947.

Lin D, Edwards AS, Fawcett JP, Mbamalu G, Scott JD, Pawson T. (2000). A mammalian PAR-3–PAR-6 complex implicated in Cdc42/Rac1 and aPKC signalling and cell polarity. *Nat Cell Biol* **2**: 540–547.

Macara IG. (2004). Parsing the polarity code. *Nat Rev Mol Cell Biol* **5**: 220–231.

Mei R, Galipeau PC, Prass C, Berno A, Ghandour G, Patil N *et al.* (2000). Genome-wide detection of allelic imbalance using human SNPs and high-density DNA arrays. *Genome Res* **10**: 1126–1137.

Nagayama K, Kohno T, Sato M, Arai Y, Minna JD, Yokota J. (2007). Homozygous deletion scanning of the lung cancer genome at a 100-kb resolution. *Genes Chromosomes Cancer* **46**: 1000–1010.

Nannya Y, Sanada M, Nakazaki K, Hosoya N, Wang L, Hangaishi A *et al.* (2005). A robust algorithm for copy number detection using high-density oligonucleotide single nucleotide polymorphism genotyping arrays. *Cancer Res* **65**: 6071–6079.

Stevenson BR, Siliciano JD, Mooseker MS, Goodenough DA. (1986). Identification of ZO-1: a high molecular weight polypeptide associated with the tight junction (zonula occludens) in a variety of epithelia. *J Cell Biol* **103**: 755–766.

Suzuki A, Ohno S. (2006). The PAR–aPKC system: lessons in polarity. *J Cell Sci* **119**: 979–987.

Vizcaino AP, Moreno V, Lambert R, Parkin DM. (2002). Time trends incidence of both major histologic types of esophageal carcinomas in selected countries, 1973–1995. *Int J Cancer* **99**: 860–868.

Wodarz A, Näthke I. (2007). Cell polarity in development and cancer. *Nat Cell Biol* **9**: 1016–1024.

Yasui K, Imoto I, Fukuda Y, Pimkhaokham A, Yang ZQ, Naruto T *et al.* (2001). Identification of target genes within an amplicon at 14q12–q13 in esophageal squamous cell carcinoma. *Genes Chromosomes Cancer* **32**: 112–118.

Zhao X, Li C, Paez JG, Chin K, Jänne PA, Chen TH *et al.* (2004). An integrated view of copy number and allelic alterations in the cancer genome using single nucleotide polymorphism arrays. *Cancer Res* **64**: 3060–3071.

Zitzelsberger H, Hieber L, Richter H, Unger K, Briscoe CV, Peddie C *et al.* (2004). Gene amplification of atypical PKC-binding PARD3 in radiation-transformed neoplastic retinal pigment epithelial cell lines. *Genes Chromosomes Cancer* **40**: 55–59.

Supplementary Information accompanies the paper on the Oncogene website (http://www.nature.com/onc)